US 20210275058A1

(19) United States

(12) Patent Application Publication (10) Pub. No.: US 2021/0275058 A1

Zia et al. (43) Pub. Date: Sep. 9, 2021

(54) **SYSTEMS AND METHODS FOR AUTOMATED LOCALIZATION OF WEARABLE CARDIAC MONITORING SYSTEMS AND SENSOR POSITION-INDEPENDENT HEMODYNAMIC INFERENCE**

(71) Applicant: **Georgia Tech Research Corporation**, Atlanta, GA (US)

(72) Inventors: **Jonathan Zia**, Atlanta, GA (US); **Omer Inan**, Atlanta, GA (US); **Jacob Kimball**, Atlanta, GA (US); **Christopher Rozell**, Atlanta, GA (US)

(21) Appl. No.: **17/316,290**

(22) Filed: **May 10, 2021**

Related U.S. Application Data

(63) Continuation-in-part of application No. 17/187,585, filed on Feb. 26, 2021, which is a continuation of application No. 16/935,882, filed on Jul. 22, 2020, now abandoned.

(60) Provisional application No. 62/877,404, filed on Jul. 23, 2019.

Publication Classification

(51) **Int. Cl.**

A61B 5/11	(2006.01)
A61B 5/00	(2006.01)
A61B 5/06	(2006.01)

(52) **U.S. Cl.**

CPC ***A61B 5/1102*** (2013.01); ***A61B 5/065*** (2013.01); ***A61B 5/7267*** (2013.01); ***A61B 5/7221*** (2013.01)

(57) **ABSTRACT**

The disclosed technology includes devices and methods for a wearable cardiac monitoring system to determine morphological variability and localization of the wearable cardiac monitoring system. The disclosed technology can include receiving seismocardiographic data, determining a classifier of the seismocardiographic data, determining a signal quality index of the seismocardiographic data, determining a quality of the seismocardiographic data based on the classifier and the signal quality index, and outputting an indication of the quality of the seismocardiographic data to a graphical user interface.

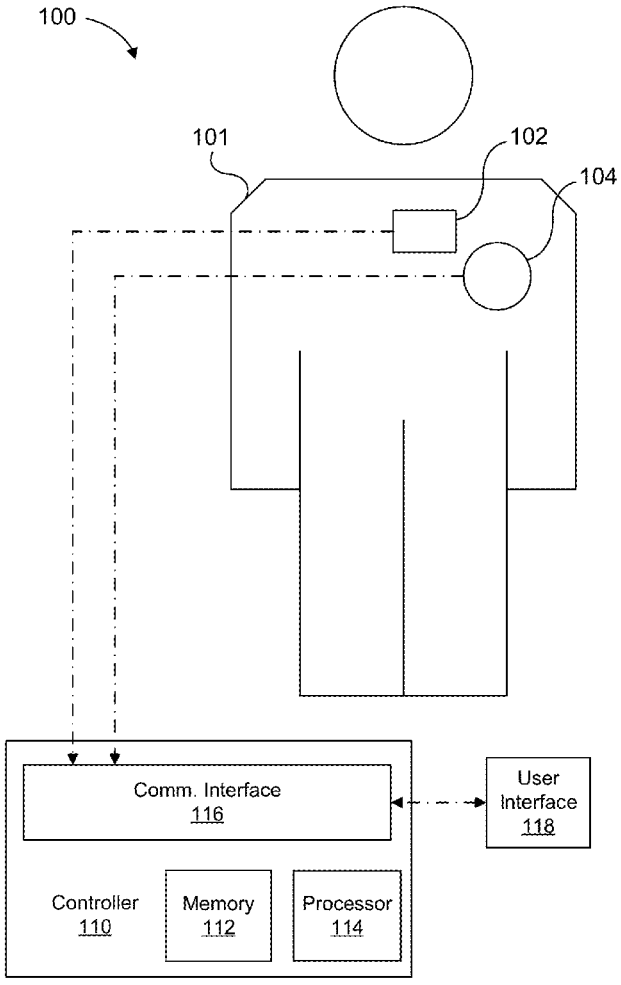

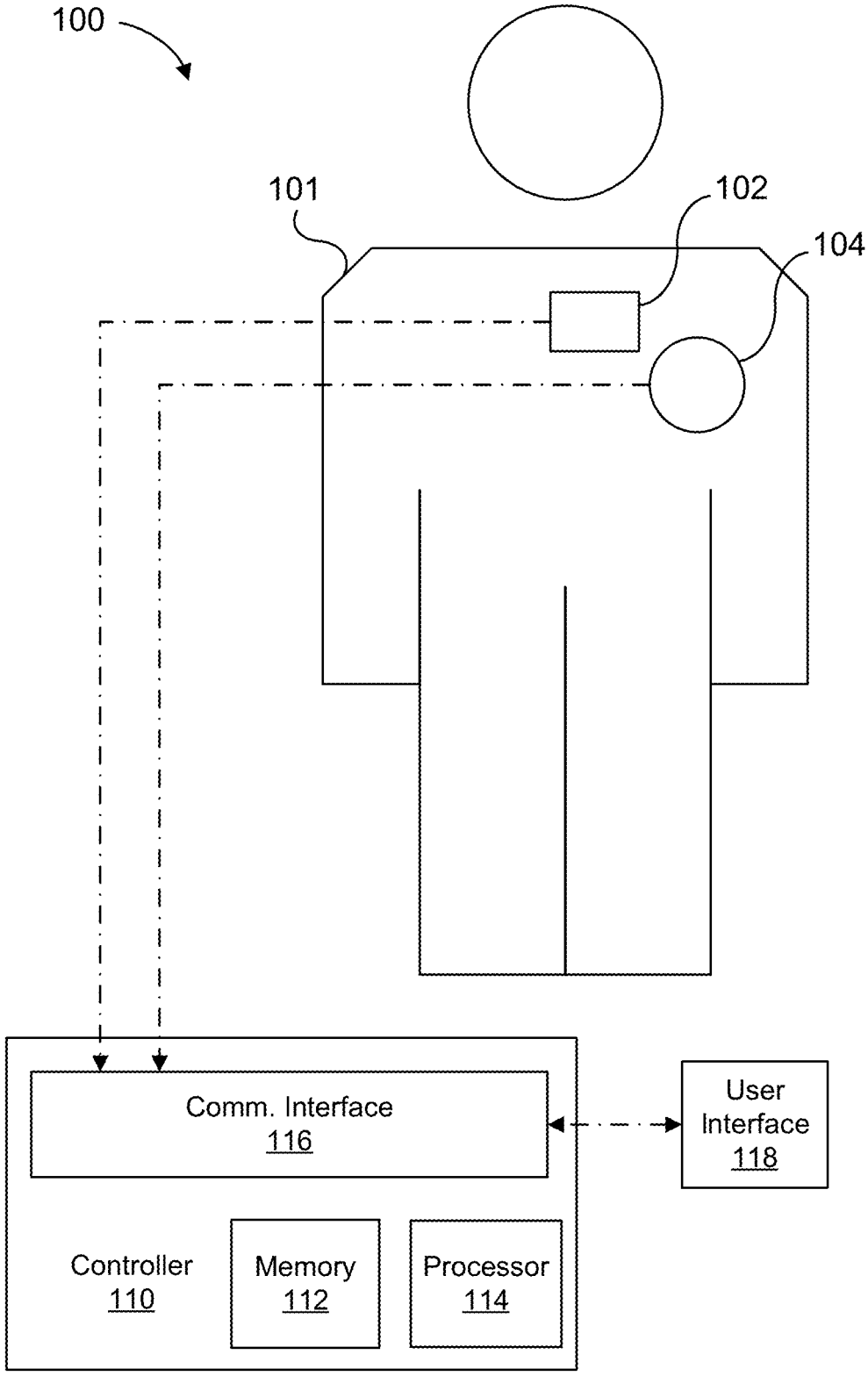
100
101
102
104
Comm. Interface
116
User
Interface
118
Controller
110
Memory
112
Processor
114

FIG. 1

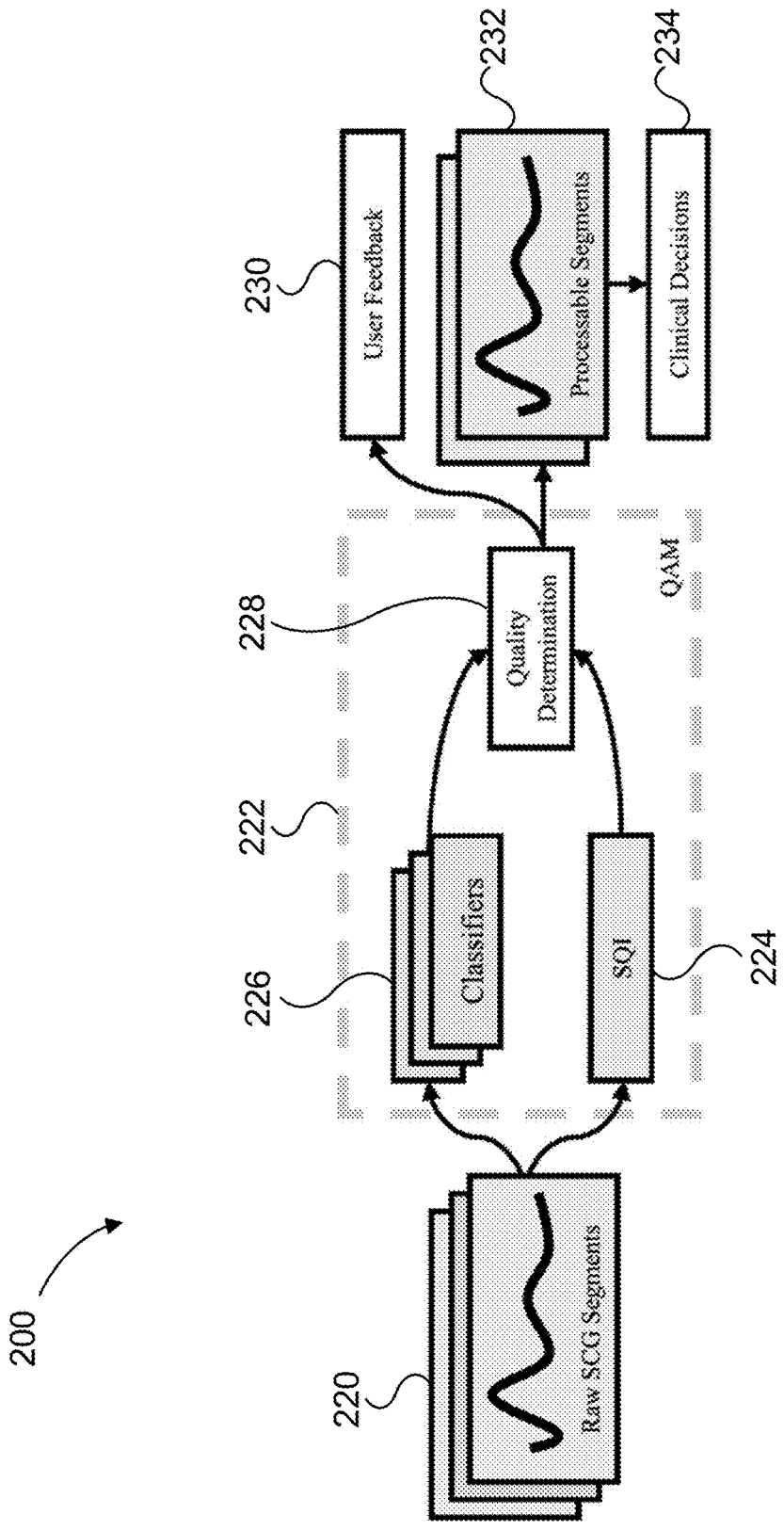
200
220
Raw SCG Segments
222
226
Classifiers
224
SQI
228
Quality Determination
QAM
230
User Feedback
232
Processable Segments
234
Clinical Decisions

FIG. 2

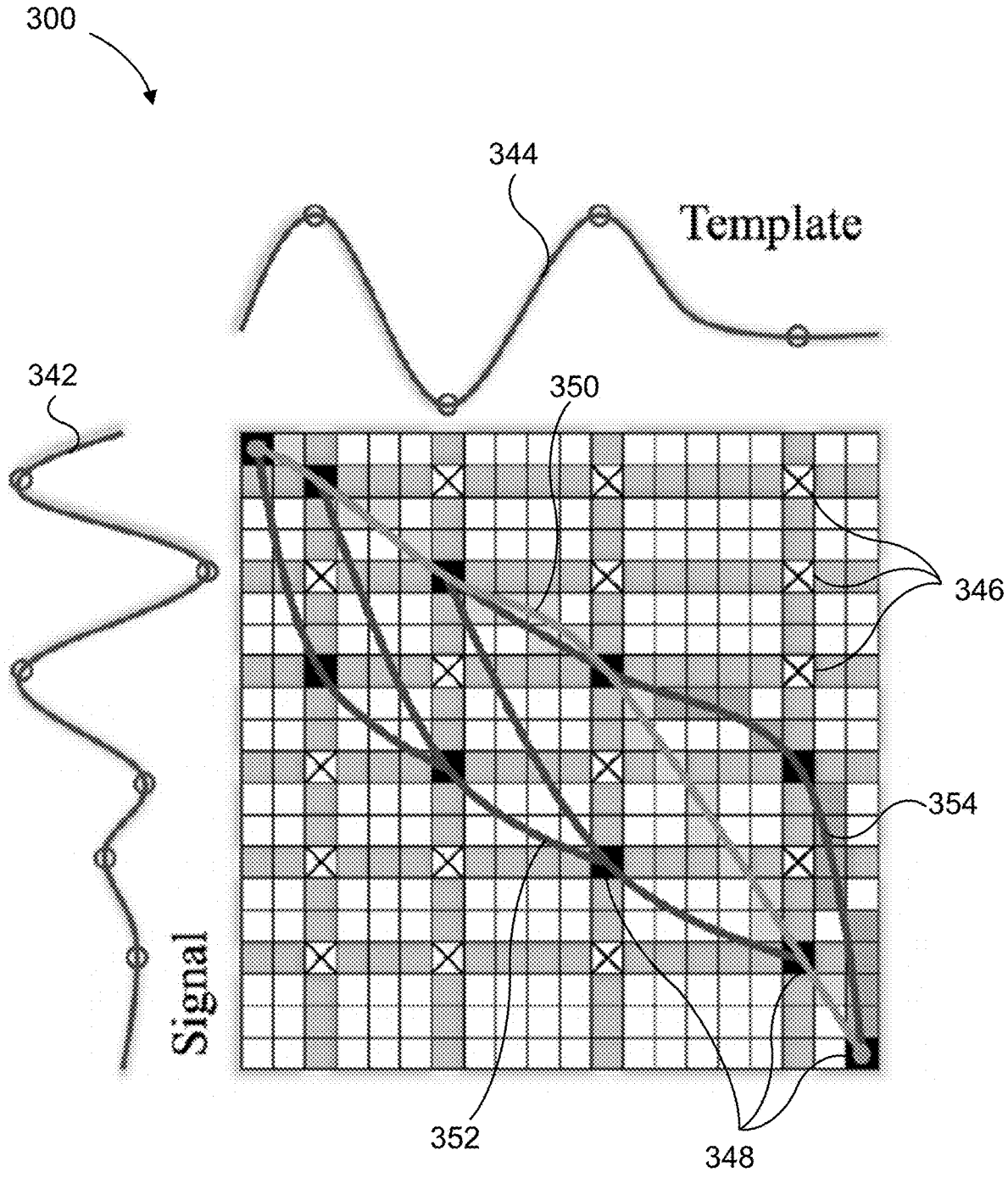

FIG. 3

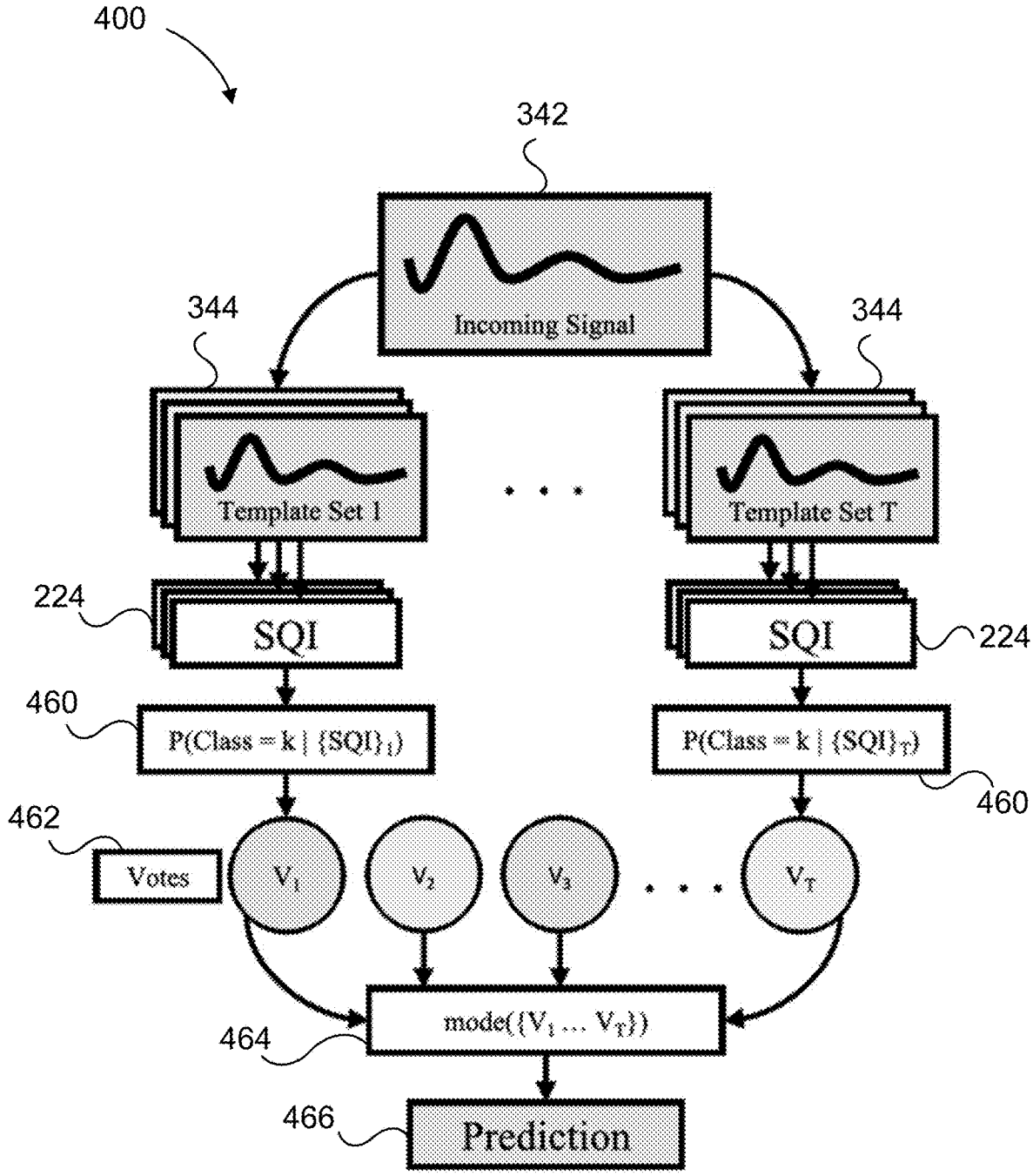
400
342
Incoming Signal
344
344
Template Set 1
Template Set T
224
SQI
SQI
224
460
P(Class = k | {SQI}1)
P(Class = k | {SQI}T)
460
462
Votes
V1
V2
V3
VT
mode({V1 ... VT})
464
466
Prediction

FIG. 4

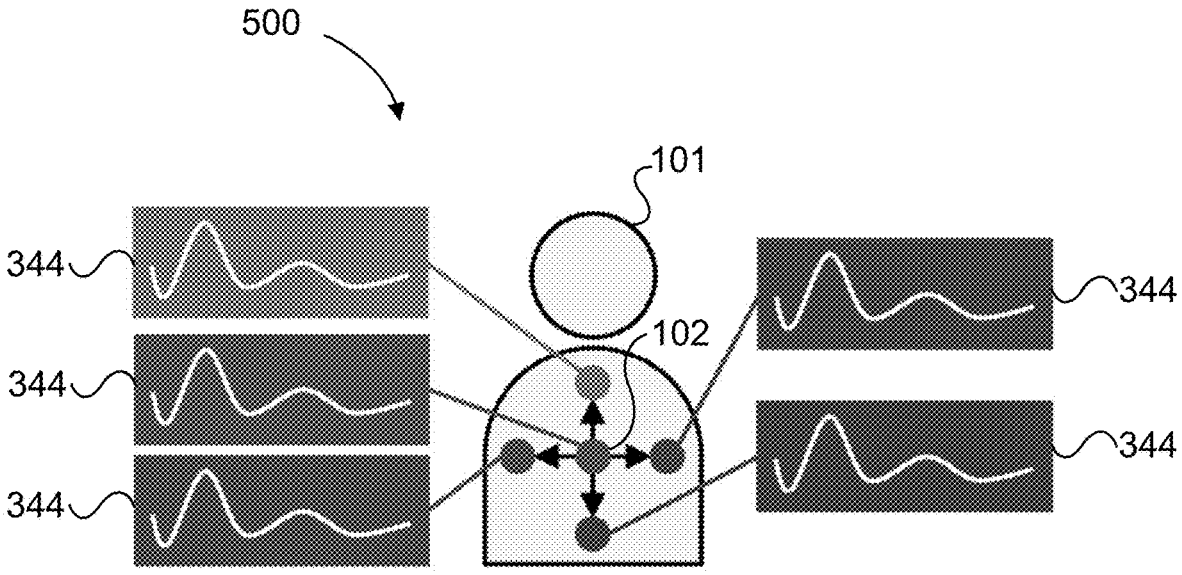
500
101
102
344
344
344
344
344

FIG. 5A

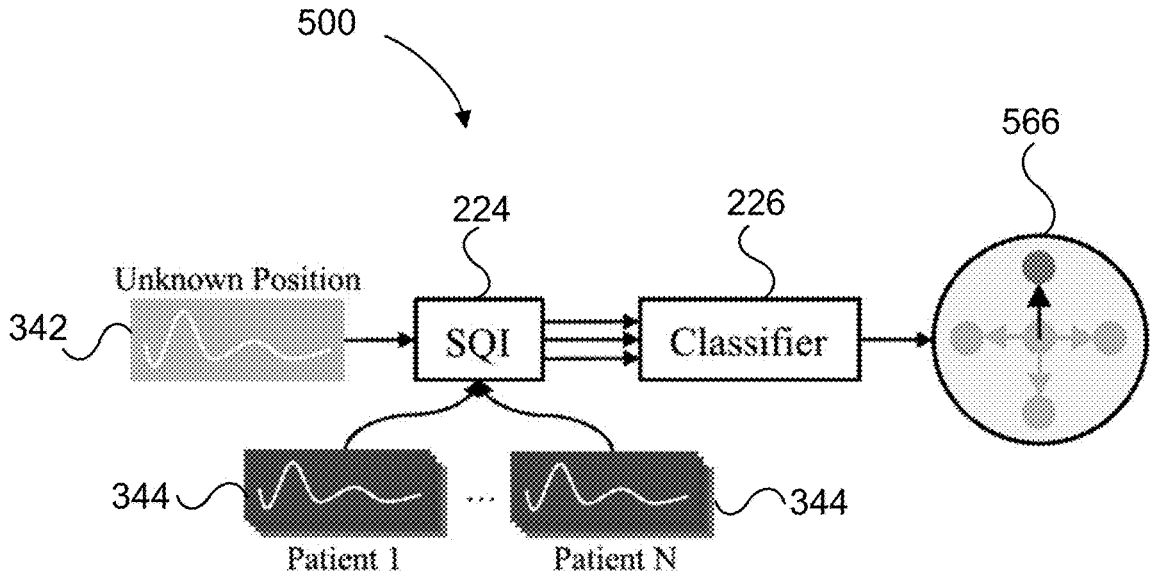
500
566
224
226
Unknown Position
342
SQI
Classifier
344
344
Patient 1
Patient N

FIG. 5B

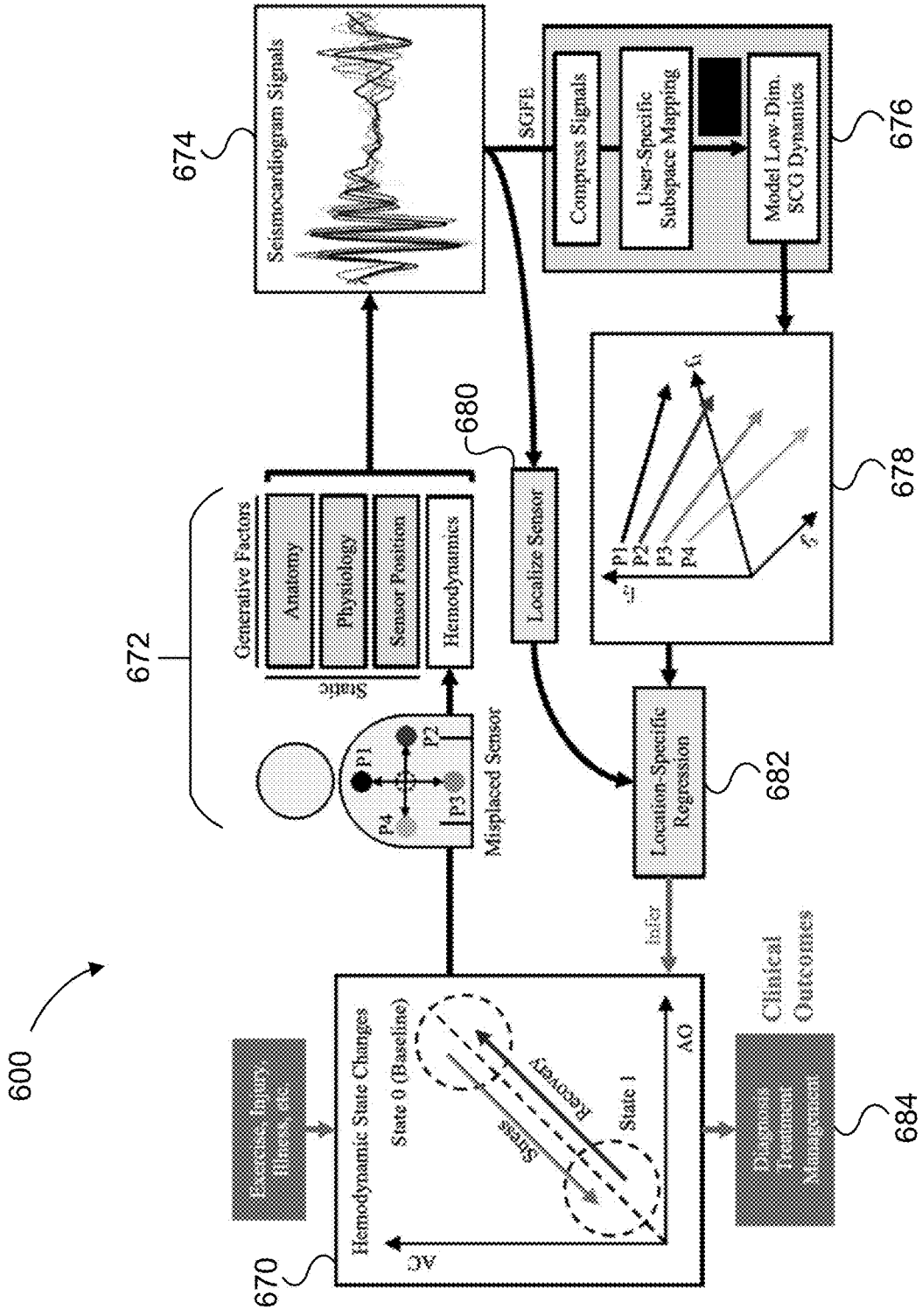
600
670
Hemodynamic State Changes
State 0 (Baseline)
State 1
Stress
Recovery
ΔC
ΔO
Initial Patient Data
Clinical Outcomes
Patient Treatment Management
684
Initial
672
Generative Factors
Anatomy
Physiology
Sensor Position
Hemodynamics
Static
Misplaced Sensor
P1
P2
P3
P4
680
Localize Sensor
682
Location-Specific Regression
674
Seismocardiogram Signals
SGFE
Compress Signals
User-Specific Subspace Mapping
Model Low-Dim. SCG Dynamics
676
678
P1
P2
P3
P4

FIG. 6

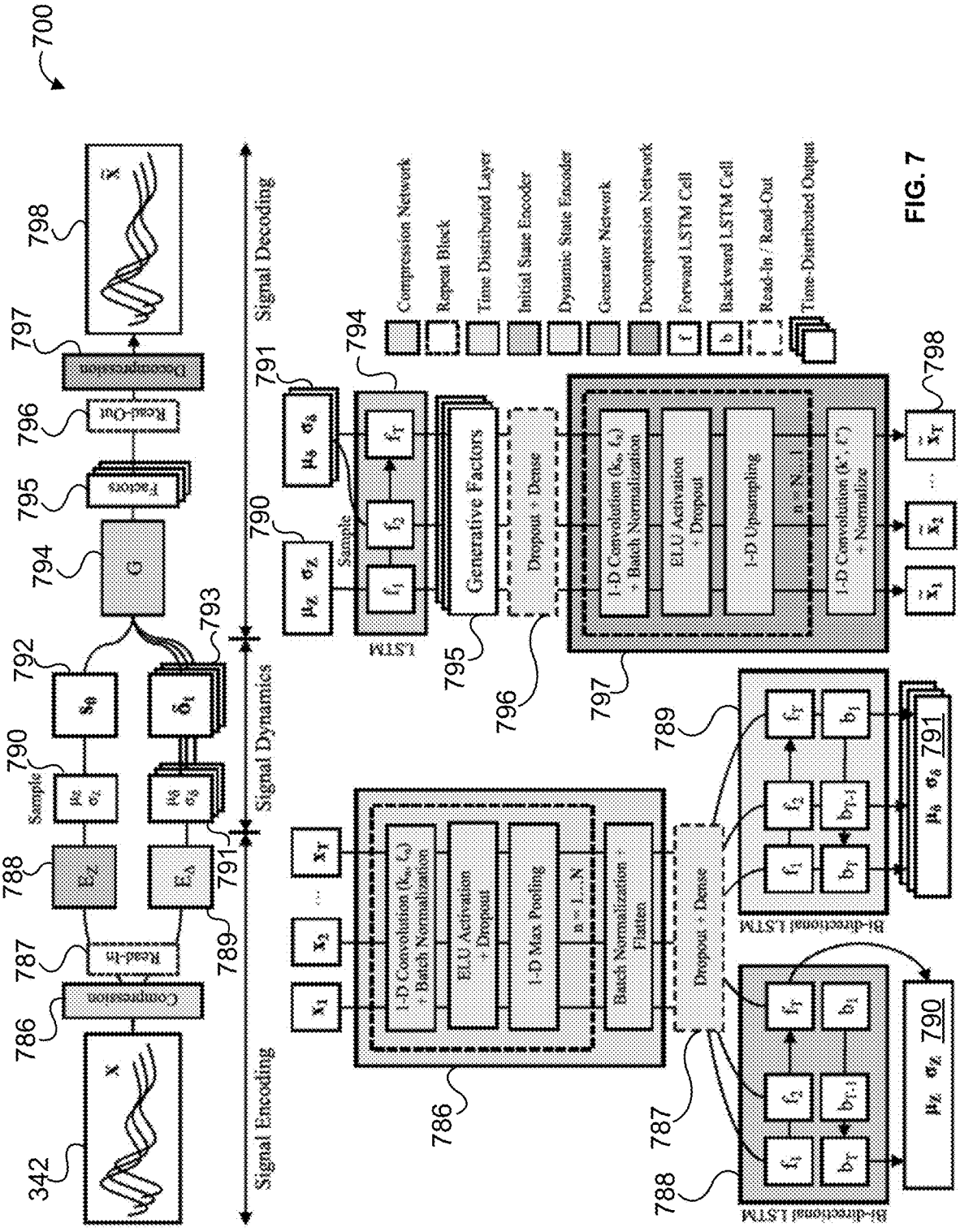
700
342
786
787
788
789
790
791
792
793
794
795
796
797
798
Signal Encoding
Signal Dynamics
Signal Decoding
Compression Network
Repeat Block
Time Distributed Layer
Initial State Encoder
Dynamic State Encoder
Generator Network
Decompression Network
Forward LSTM Cell
Backward LSTM Cell
Read-In / Read-Out
Time-Distributed Output
Generative Factors
Dropout + Dense
Sample
LSTM
Bi-directional LSTM
1-D Convolution + Batch Normalization
ELU Activation + Dropout
1-D Max Pooling
Batch Normalization + Flatten
1-D Upsampling
1-D Convolution + Normalize

FIG. 7

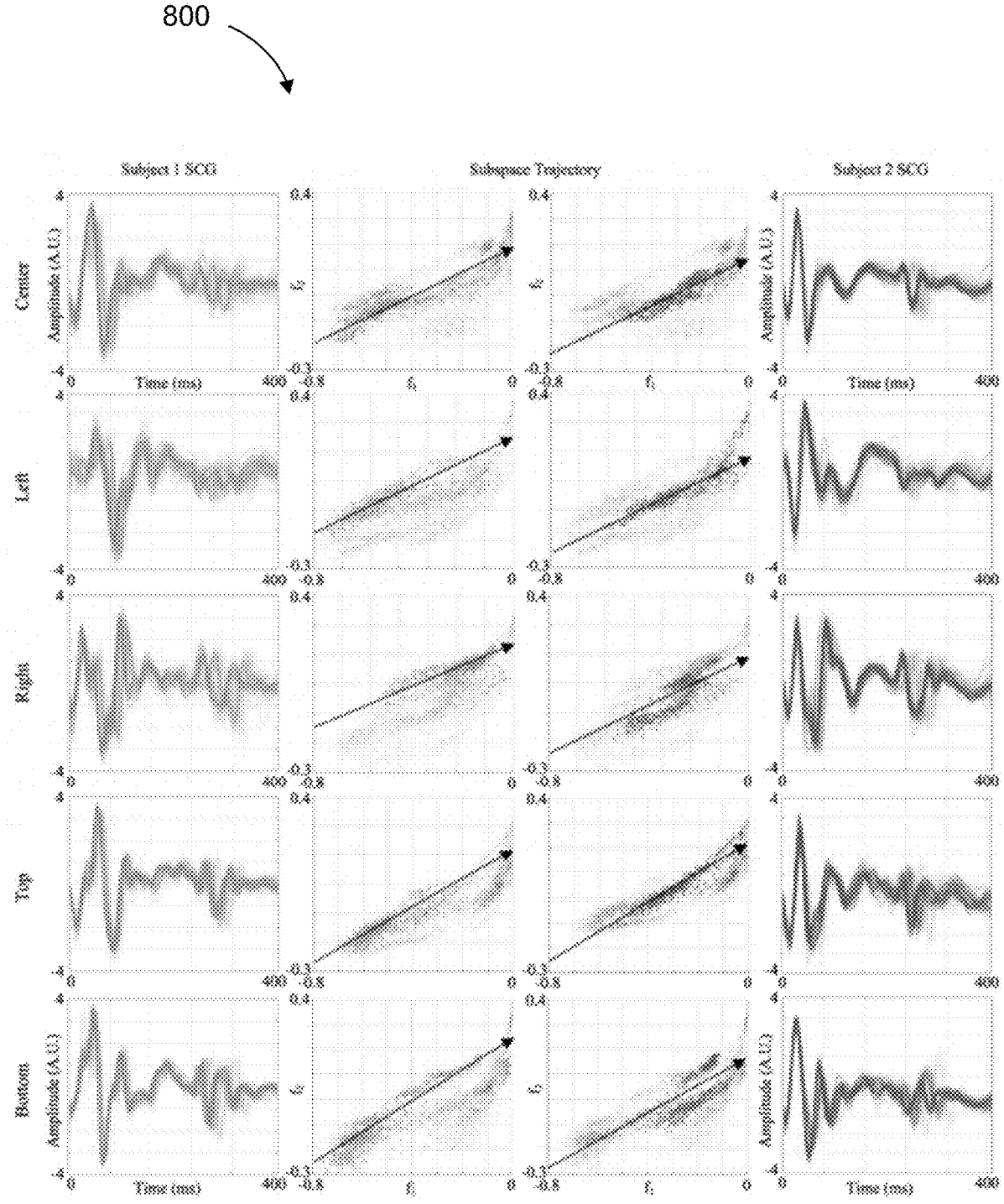
800
Subject 1 SCG
Subspace Trajectory
Subject 2 SCG
Center
Left
Right
Top
Bottom
Amplitude (A.U.)
Time (ms)

FIG. 8

FIG. 9A

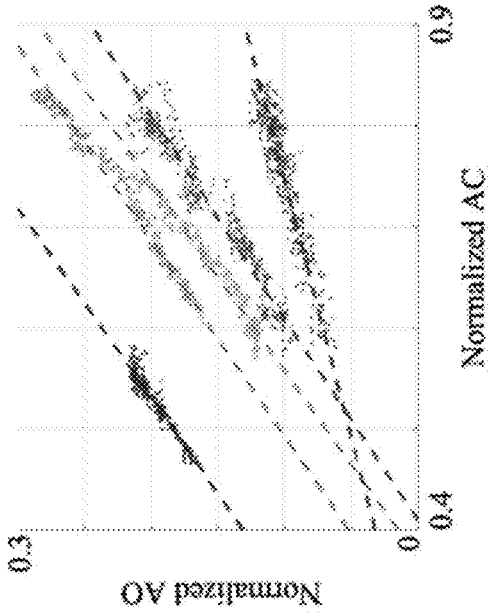

FIG. 9B

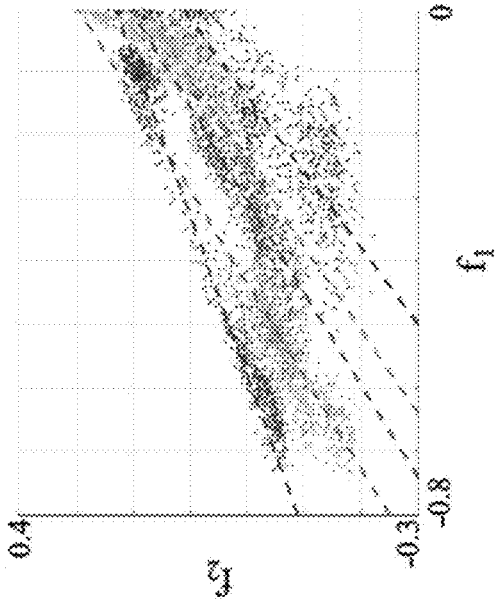

FIG. 9C

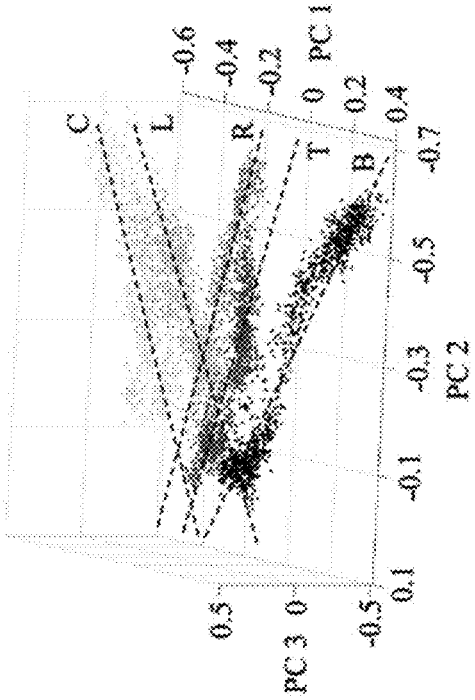

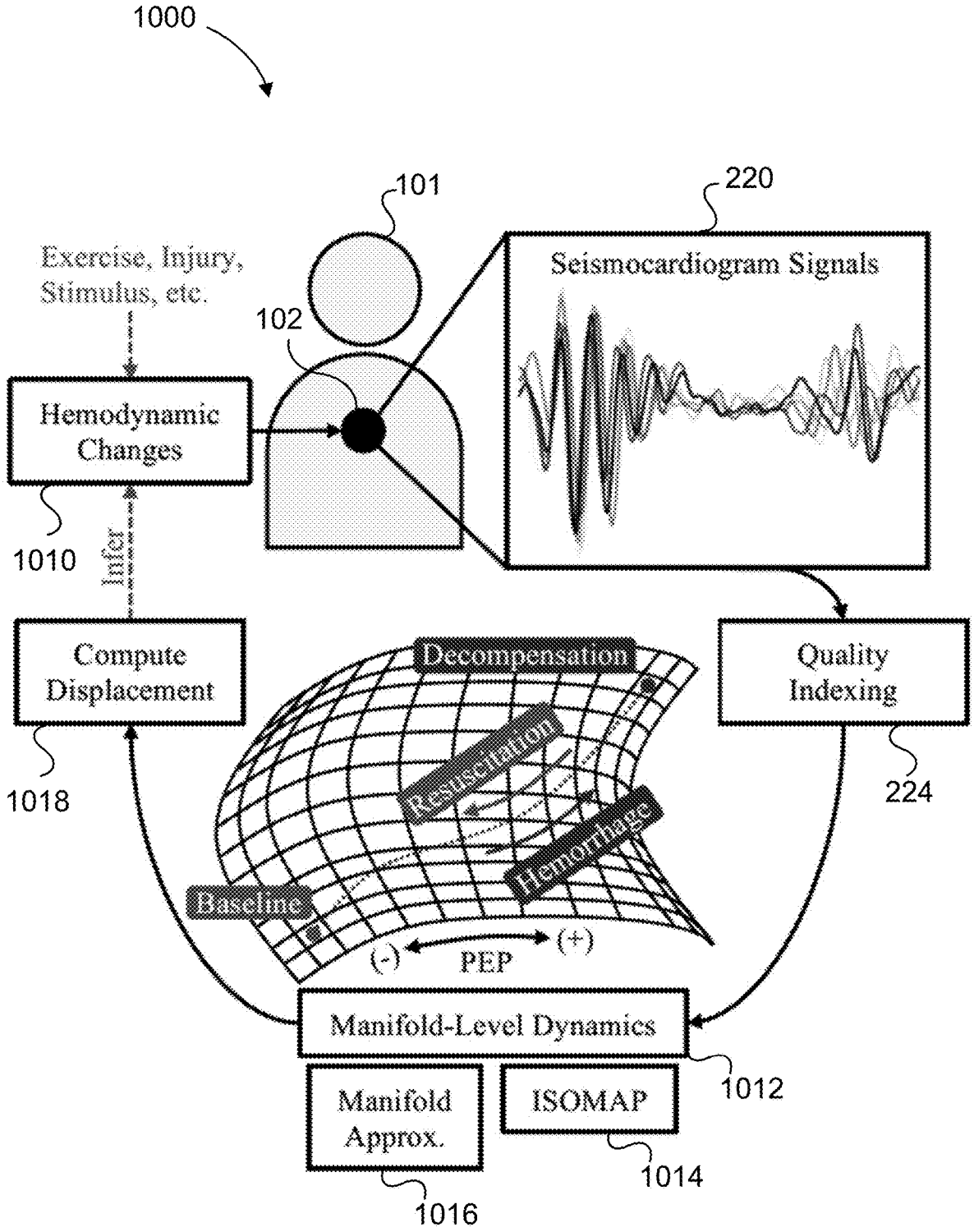
1000
101
220
Exercise, Injury, Stimulus, etc.
102
Seismocardiogram Signals
Hemodynamic Changes
1010
Infer
Compute Displacement
1018
Quality Indexing
224
Decompensation
Resuscitation
Hemorrhage
Baseline
(-)
PEP
(+)
Manifold-Level Dynamics
1012
Manifold Approx.
1016
ISOMAP
1014

FIG. 10

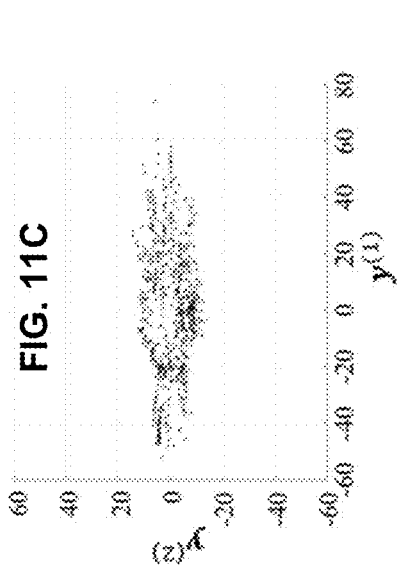

FIG. 11C

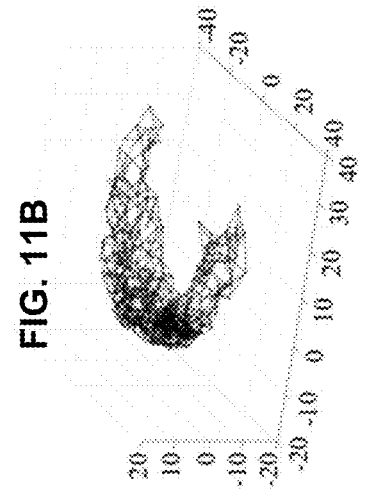

FIG. 11B

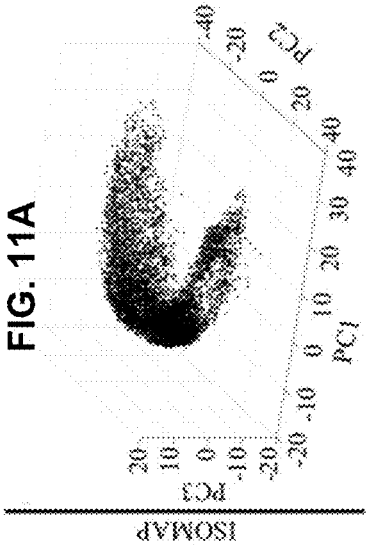

FIG. 11A

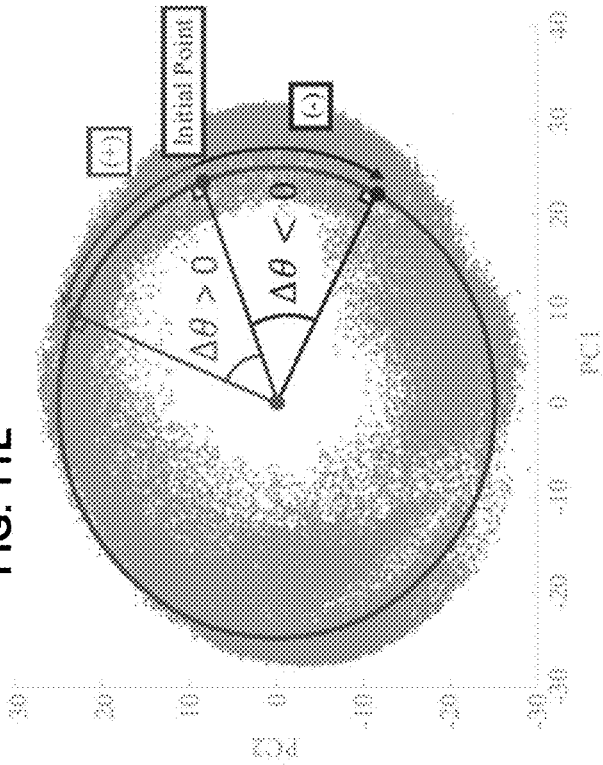

FIG. 11E

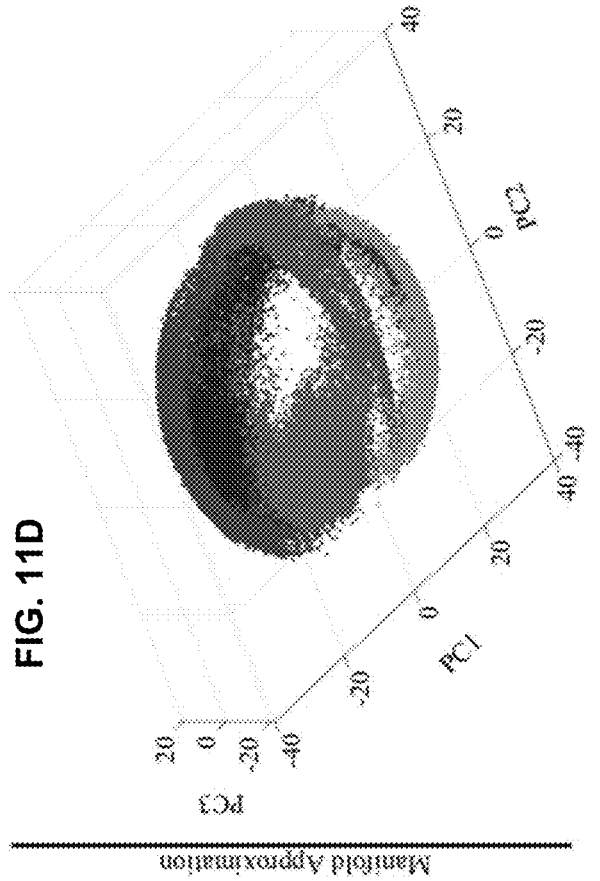

FIG. 11D

SYSTEMS AND METHODS FOR AUTOMATED LOCALIZATION OF WEARABLE CARDIAC MONITORING SYSTEMS AND SENSOR POSITION-INDEPENDENT HEMODYNAMIC INFERENCE

CROSS-REFERENCE TO RELATED APPLICATIONS

[0001] This application is a continuation-in-part of U.S. patent application Ser. No. 17/187,585, filed 26 Feb. 2021, which is a continuation of U.S. patent application Ser. No. 16/935,882, filed 22 Jul. 2020, which claims the benefit of U.S. Provisional Patent Application No. 62/877,404 filed 23 Jul. 2019, each of which is hereby incorporated by reference as if fully set forth below.

STATEMENT REGARDING GOVERNMENT SUPPORT

[0002] This invention was made with government support under Award No. 1R01HL134619-A1 awarded by the National Institutes of Health and UL1TR002378 awarded by the National Center for Advancing Translational Sciences. The government has certain rights in the invention.

FIELD OF DISCLOSURE

[0003] The disclosed technology relates generally to wearable cardiac monitoring systems and, more particularly, to systems and methods for automated localization of wearable cardiac monitoring systems and generation of physiological inferences using wearable cardiac monitoring systems measuring precordial acceleration.

BACKGROUND

[0004] Seismocardiography is a technique of measuring the movement of the chest wall in response to underlying cardiovascular events. Seismocardiography, for example, can be used to measure valvular events such as aortic opening (AO) and aortic closing (AC). Data collected by seismocardiography can be compiled into a seismocardiogram to enable medical professionals to make an inference of major prognostic factors of heart disease such as pre-ejection period (PEP), left ventricular ejection time (LVET), and pulse transit time (PTT).

[0005] By its nature, the morphology of a seismocardiographic (SCG) waveform is highly transient in the time domain, influenced by the coupling of the vascular system with the chest wall, the chest wall with the sensing system, and by the patient's physiological state. Consequently, morphological variability poses a significant challenge in processing SCG signals. Furthermore, when a seismocardiography signal is obtained by the sensing system, the information extracted from the obtained signal can vary significantly based on where the sensor is placed; thus, misplacement of the sensor can lead to readings that are not reliable. This is particularly a problem when a seismocardiogram is used during outpatient continuous monitoring because the patient typically is not trained to properly position the wearable sensor and because the wearable sensor can be knocked out of position while worn by the patient. These variations associated with obtaining and recording an SCG signal pose significant challenges for professionals to determine whether the obtained bio-signal, and any resultant seismocardiogram, is of sufficient quality to be used in informing patient care. Oftentimes, the challenges in properly positioning the wearable sensor render the sensor, and information it obtains, useless because the underlying processing system cannot properly account for the misplacement of the sensors.

[0006] What is needed, therefore, is a system and method that can determine a location of the sensor on the chest wall and correct distortions of extracted sensor information resulting from sensor misplacement or morphological variations, thus providing an accurate seismocardiogram based on the detected SCG signals.

SUMMARY

[0007] These and other problems can be addressed by the technologies described herein. Examples of the present disclosure relate generally to systems and methods for automated morphological variability detection and localization of wearable cardiac monitoring systems measuring precordial acceleration.

[0008] The disclosed technology can include a method of detecting morphological changes using a wearable cardiac monitor. The method can include receiving seismocardiographic data from a motion sensor and determining, based at least in part on the seismocardiographic data, a classifier of the seismocardiographic data. The method can include determining, based at least in part on the seismocardiographic data, a signal quality index of the seismocardiographic data and determining, based on the classifier and the signal quality index, a quality of the seismocardiographic data. The method can further include outputting, to a graphical user interface, the quality of the seismocardiographic data.

[0009] The classifier can include multiple classifiers and the method can include performing ensemble prediction by utilizing the multiple classifiers to create an ensemble classifier. The method can also include retrieving a reference template and determining the signal quality index by determining a distance between the seismocardiographic data and the reference template. The reference template can be representative of seismocardiographic data.

[0010] The method can include estimating the distance between the seismocardiographic data and the reference template by dynamic-time feature matching. Dynamic-time feature matching can include determining a local minimum and a local maximum of the seismocardiographic data and determining a local minimum and a local maximum of the reference template. The method can include determining a prohibited intersection point, determining a candidate point, and generating a warp path through the candidate point.

[0011] The method can include retrieving a location-specific reference template and determining a location of the motion sensor by at least determining a distance between the seismocardiographic data and the location-specific reference template. The location-specific reference template can be representative seismocardiographic data at a predetermine location.

[0012] The method can include determining a hemodynamic factor by modeling the seismocardiographic data as a stochastic sample from an underlying dynamical system. The method can include performing a seismocardiogram generative factor encoding, comparing the seismocardiographic data to a low-dimensional subspace, and applying a position-specific regression to the low-dimensional subspace to determine a hemodynamic factor.

[0013] The method can include comparing the seismocardiographic data to a low-dimensional manifold, performing a manifold approximation to analyze a distance traveled along the low-dimensional manifold, and determining a hemodynamic change based on the distance traveled along the low-dimensional manifold.

[0014] The disclosed technology can include a wearable cardiac monitoring system that can include a controller and a motion sensor configured to detect movement of a user's chest and output seismocardiographic data to the controller. The controller can include a non-transitory, computer-readable medium having instructions stored thereon that, when executed by one or more processors, cause a controller to receive the seismocardiographic data from the motion sensor and determine, based at least in part on the seismocardiographic data, a classifier of the seismocardiographic data. The instructions can cause the controller to determine, based at least in part on the seismocardiographic data, a signal quality index of the seismocardiographic data and determine, based on the classifier and the signal quality index, a quality of the seismocardiographic data. The instructions can cause the controller to output, to a graphical user interface, an indication of the quality of the seismocardiographic data.

[0015] The classifier can comprise a property of a source distribution of the seismocardiographic data. The classifier can comprise multiple classifiers and the instructions, when executed by the one or more processors, can cause the controller to perform ensemble prediction by utilizing the multiple classifiers to create an ensemble classifier.

[0016] The instructions can further cause the controller to retrieve a reference template and determine the signal quality index by determining a distance between the seismocardiographic data and the reference template. The reference template can be representative of seismocardiographic data. The instructions can further cause the controller to estimate the distance between the seismocardiographic data and the reference template by dynamic-time feature matching. The dynamic-time feature matching can include determining a local minimum and a local maximum of the seismocardiographic data and determining a local minimum and a local maximum of the reference template. Dynamic-time feature matching can include determining a prohibited intersection point, determining a candidate point, and generating a warp path through the candidate point.

[0017] The instructions can further cause the controller to retrieve a location-specific reference template and determine a location of the motion sensor by at least determining a distance between the seismocardiographic data and the location-specific reference template. The location-specific reference template can be representative seismocardiographic data at a predetermine location.

[0018] The instructions can cause the controller to perform a seismocardiogram generative factor encoding, compare the seismocardiographic data to a low-dimensional subspace, and apply a position-specific regression to the low-dimensional subspace to determine a hemodynamic factor.

[0019] The instructions can further cause the controller to compare the seismocardiographic data to a low-dimensional manifold, perform a manifold approximation to analyze a distance traveled along the low-dimensional manifold, and determine a hemodynamic change based on the distance traveled along the low-dimensional manifold.

[0020] The controller can be configured to wirelessly receive the seismocardiographic data from the motion sensor. The controller can be a remote server configured to wirelessly receive the seismocardiographic data from the motion sensor. The controller can be integrated with the motion sensor into a single wearable device.

[0021] The instructions can cause the controller to receive a first input to change a threshold value of the classifier and receive a second input to change a threshold value of the signal quality index.

[0022] Additional features, functionalities, and applications of the disclosed technology are discussed herein in more detail.

BRIEF DESCRIPTION OF THE FIGURES

[0023] The accompanying drawings, which are incorporated in and constitute a part of this specification, illustrate various aspects of the presently disclosed subject matter and serve to explain the principles of the presently disclosed subject matter. The drawings are not intended to limit the scope of the presently disclosed subject matter in any manner.

[0024] FIG. **1** is an illustration of a wearable cardiac monitoring system, in accordance with the disclosed technology.

[0025] FIG. **2** is an illustration of a method of analyzing seismocardiogram signals, in accordance with the disclosed technology.

[0026] FIG. **3** is graph of analyzed seismocardiogram signals, in accordance with the disclosed technology.

[0027] FIG. **4** is an illustration of a method of analyzing seismocardiogram signals, in accordance with the disclosed technology.

[0028] FIG. **5**A is an illustration of various sensor locations, in accordance with the disclosed technology.

[0029] FIG. **5**B is an illustration of a method of analyzing seismocardiogram signals and determining a location of a sensor, in accordance with the disclosed technology.

[0030] FIG. **6** is an illustration of a method of analyzing seismocardiogram signals, in accordance with the disclosed technology.

[0031] FIG. **7** is an illustration of a method of analyzing seismocardiogram signals, in accordance with the disclosed technology.

[0032] FIG. **8** illustrates various graphs of seismocardiogram signals in accordance with the disclosed technology.

[0033] FIGS. **9**A-**9**C illustrates various graphs of seismocardiogram signals in accordance with the disclosed technology.

[0034] FIG. **10** is an illustration of a method of analyzing seismocardiogram signals, in accordance with the disclosed technology.

[0035] FIGS. **11**A-**11**E illustrates various graphs of seismocardiogram signals in accordance with the disclosed technology.

DETAILED DESCRIPTION

[0036] The disclosed technology relates to improved systems and methods for automated morphological variability detection and localization of wearable cardiac monitoring systems measuring precordial acceleration. The disclosed technology can include wearable cardiac monitors (e.g., holter monitors and other wearable devices that capture

cardiovascular data such as electrocardiograph (ECG)) that incorporate sensors used to capture signals that can be processed to create seismocardiograms and the underlying processing systems to both (1) localize the sensor and (2) correct for sensor misplacement and morphological variability when inferring AO and AC event timing from the signal. The disclosed technology can greatly improve the user experience when using the wearable cardiac monitors because the user is not required to place the sensor in a single specific location on his or her chest. Furthermore, the disclosed technology includes methods for extracting biosignal data independently of waveform morphology to yield more consistent data when applied to a heterogeneous population, which is essential in ambulatory and outpatient environments.

[0037] As will become apparent throughout this disclosure, the disclosed technology can include systems and methods for improving sensor localization by using, among other things, a variant of dynamic time warping (DTW) called dynamic time feature matching (DTFM) to infer sensor location from seismocardiography signals using ensembled quadratic discriminant analysis (QDA) classification. Furthermore, the disclosed technology can include dynamic systems modeling used to correct estimated AO and AC values based on the location of the sensor once the sensor has been localized. Combining these methods can yield a system which both localizes the wearable sensor on the chest wall and corrects distortions of extracted sensor information resulting from sensor misplacement. In other words, the disclosed technology can enable position-specific mapping of seismocardiographic data to infer hemodynamic variables. By localizing the sensor, the disclosed technology can be used either to inform the patient where to properly place the sensor on his or her chest or to automatically compensate for the sensor misplacement without requiring the sensor to be relocated.

[0038] Although various aspects of the disclosed technology are explained in detail herein, it is to be understood that other aspects of the disclosed technology are contemplated. Accordingly, it is not intended that the disclosed technology is limited in its scope to the details of construction and arrangement of components expressly set forth in the following description or illustrated in the drawings. The disclosed technology can be implemented and practiced or carried out in various ways. In particular, the presently disclosed subject matter is described in the context of being systems and methods for automated localization and misplacement correction of wearable cardiac monitoring systems measuring precordial acceleration. The present disclosure, however, is not so limited, and can be applicable in other contexts. Accordingly, when the present disclosure is described in the context of automated localization and misplacement correction of wearable cardiac monitoring systems measuring precordial acceleration, it will be understood that other implementations can take the place of those referred to.

[0039] It should also be noted that, as used in the specification and the appended claims, the singular forms "a," "an," and "the" include plural references unless the context clearly dictates otherwise. References to a composition containing "a" constituent is intended to include other constituents in addition to the one named.

[0040] Also, in describing the disclosed technology, terminology will be resorted to for the sake of clarity. It is intended that each term contemplates its broadest meaning as understood by those skilled in the art and includes all technical equivalents which operate in a similar manner to accomplish a similar purpose.

[0041] Ranges may be expressed herein as from "about" or "approximately" or "substantially" one particular value and/or to "about" or "approximately" or "substantially" another particular value. When such a range is expressed, the disclosed technology can include from the one particular value and/or to the other particular value. Further, ranges described as being between a first value and a second value are inclusive of the first and second values. Likewise, ranges described as being from a first value and to a second value are inclusive of the first and second values.

[0042] Herein, the use of terms such as "having," "has," "including," or "includes" are open-ended and are intended to have the same meaning as terms such as "comprising" or "comprises" and not preclude the presence of other structure, material, or acts. Similarly, though the use of terms such as "can" or "may" are intended to be open-ended and to reflect that structure, material, or acts are not necessary, the failure to use such terms is not intended to reflect that structure, material, or acts are essential. To the extent that structure, material, or acts are presently considered to be essential, they are identified as such.

[0043] It is also to be understood that the mention of one or more method steps does not preclude the presence of additional method steps or intervening method steps between those steps expressly identified. Moreover, although the term "step" can be used herein to connote different aspects of methods employed, the term should not be interpreted as implying any particular order among or between various steps herein disclosed unless and except when the order of individual steps is explicitly required. Further, the disclosed technology does not necessarily require all steps included in the methods and processes described herein. That is, the disclosed technology includes methods that omit one or more steps expressly discussed with respect to the methods described herein.

[0044] The components described hereinafter as making up various elements of the disclosed technology are intended to be illustrative and not restrictive. Many suitable components that would perform the same or similar functions as the components described herein are intended to be embraced within the scope of the disclosed technology. Such other components not described herein can include, but are not limited to, similar components that are developed after development of the presently disclosed subject matter.

[0045] Referring now to the drawings, in which like numerals represent like elements, the present disclosure is herein described. FIG. **1** illustrates a system **100** for, among other things, automated morphological variability detection and localization of wearable cardiac monitoring systems measuring precordial acceleration. The system **100** can include a motion sensor **102** and an electrical activity sensor **104** that can be worn by, or otherwise placed on, a patient **101**. The motion sensor **102** and the electrical activity sensor **104** can both be configured to output a detected signal to a controller **110**. As will be described in greater detail herein, the controller **110** can be configured to receive data from the motion sensor **102** and the electrical activity sensor **104**, analyze the received data, and output data to a user interface **118** so that the patient **101**, doctor, nurse, technician, and/or

any other medical professional is able to make decisions about the patient's **101** health.

[0046] The motion sensor **102** can be any type of sensor configured to detect movement of the patient's **101** chest or body caused by underlying cardiovascular events and output motion signals (referred to herein as a seismocardiographic (SCG) signal) indicative of the detected movement. The motion sensor **102**, for example, can be an accelerometer, a three-axis accelerometer, a gyroscope (or gyrometer), an inertial measurement unit (IMU), or any other suitable type of sensor that can detect movement of the patient's **101** chest or body. The electrical activity sensor **104** can be any type of sensor configured to detect electrical activity of the patient's **101** body and output electrical activity signals that can be used to produce an electrocardiogram (ECG) and/or an impedance cardiogram (ICG). The electrical activity sensor **104** can include electrodes placed on the skin of the patient **101** that are capable of detecting electrical changes that are produced by the patient's **101** heart.

[0047] Although depicted as being two separate sensors, the motion sensor **102** and the electrical activity sensor **104** can both be mounted into a single unit such that the motion sensor **102** and the electrical activity sensor **104** comprise a single device. Furthermore, although depicted as being in communication with the controller **110** that is separate from the patient **101**, the controller **110** can be integrated with the motion sensor **102** and the electrical activity sensor **104** such that the controller **110**, the motion sensor **102**, and the electrical activity sensor **104** comprise a single unit. Alternatively, portions of the controller **110** can be integrated with the motion sensor **102** and/or the electrical activity sensor **104** while other portions of the controller **110** can be separated from the motion sensor **102** and the electrical activity sensor **104**. For example, a memory **112** and a processor **114** of the controller **110** can be integrated with the motion sensor **102** and the electrical activity sensor **104** to perform some of the actions described herein while further actions are performed by the controller **110** that is remote from the motion sensor **102** and the electrical activity sensor **104**. If the controller **110**, or portions of the controller **110** are separated from the motion sensor **102** and the electrical activity sensor **104**, the motion sensor **102** and the electrical activity sensor **104** can either be in wireless communication or wired communication with the controller **110**.

[0048] The controller **110** can have a memory **112**, a processor **114**, and a communication interface **116**. The controller **110** can be a computing device (e.g., a desktop, a laptop, a tablet, a mobile device, a remote server, or any other suitable type of computing device) configured to receive biometric data from the motion sensor **102** the electrical activity sensor **104**. One of skill in the art will appreciate that the controller **110** can be installed in any location, provided the controller **110** is in communication with at least some of the components of the system **100** (including the motion sensor **102** and the electrical activity sensor **104**). Furthermore, the controller **110** can be configured to send and receive wireless or wired signals and the signals can be analog or digital signals. The wireless signals can include Bluetooth™, BLE, WiFi™, ZigBee™, infrared, microwave radio, or any other type of wireless communication as may be suitable for the particular application. The hard-wired signal can include any directly wired connection between the controller and the other components. The digital connection can include a connection such as an Ethernet or a serial connection and can utilize any suitable communication protocol for the application such as Modbus, fieldbus, PROFIBUS, SafetyBus p, Ethernet/IP, or any other suitable communication protocol for the application. Furthermore, the controller **110** can utilize a combination of wireless, hard-wired, and analog or digital communication signals to communicate with and control the various components. One of skill in the art will appreciate that the above configurations are given merely as non-limiting examples and the actual configuration can vary depending on the particular application.

[0049] The controller **110** can include a memory **112** that can store a program and/or instructions associated with the functions and methods described herein and can include one or more processors **114** configured to execute the program and/or instructions. The memory **112** can include one or more suitable types of memory (e.g., volatile or non-volatile memory, random access memory (RAM), read only memory (ROM), programmable read-only memory (PROM), erasable programmable read-only memory (EPROM), electrically erasable programmable read-only memory (EEPROM), magnetic disks, optical disks, floppy disks, hard disks, removable cartridges, flash memory, a redundant array of independent disks (RAID), and the like) for storing files including the operating system, application programs (including, for example, a web browser application, a widget or gadget engine, and or other applications, as necessary), executable instructions and data. One, some, or all of the processing techniques or methods described herein can be implemented as a combination of executable instructions and data within the memory.

[0050] The controller **110** can also have a communication interface **116** for sending and receiving communication signals between the various components. Communication interface **116** can include hardware, firmware, and/or software that allows the processor(s) **114** to communicate with the other components via wired or wireless networks, whether local or wide area, private or public, as known in the art. Communication interface **116** can also provide access to a cellular network, the Internet, a local area network, or another wide-area network as suitable for the particular application.

[0051] Additionally, the controller **110** can have or be in communication with a user interface **138** for displaying system information and receiving inputs from a user. The user interface **138** can be installed locally on the system **100** or be a remotely controlled device such as a mobile device. The user, for example, can input data to set one or more thresholds used by the controller **110** to determine actions based on system **100** conditions.

[0052] FIG. **2** illustrates a method **200** of determining a quality of an SCG signal as detected by at least the motion sensor **102**. As illustrated in FIG. **2**, the method can include receiving SCG signal segments **220** and performing a quality assessment on the received SCG signal segments **220** at a quality assessment module **222**. The SCG signal segments **220** can include motion signals generated by the sensor **102** in response to detecting movement of the patient's **101** chest resulting from both precordial acceleration and the patient's **101** movement. The SCG signal segments **220** can be processed by a bandpass filter (e.g., 1-40 Hz) and/or some other blind source separation to help isolate the data indicative of precordial acceleration from the data indicative of movement of the patient's **101** chest. The quality assessment

module **222**, as will be explained in greater detail herein, can be configured to determine a signal quality index (SQI) **224** and classifiers **226** of the received signal segments **220** to generate a quality determination **228**. The information generated as part of the quality determination **228** can then be used by a medical professional to determine whether the received SCG data (i.e., the SCG signal segments **220**) are of sufficient quality to make determinations of the patient's **101** health. As further show in in FIG. **2**, the method **200** can include generating user feedback **230** based on the quality determination **228**, and outputting that feedback to provide the user with information about the signal quality. For example, the feedback **230** can be outputted for display on the user's computing device or a display of the system **100**, and the feedback **230** can include information indicating whether the motion sensor **102** and/or electrical activity sensor **104** is properly positioned, whether the signal is of sufficient quality to use for making informed health decisions, and information about how the user can obtain a signal of higher quality. If the quality determination **228** indicates that the signal quality is sufficient, the method **200** can further include analyzing processable segments **232** of the SCG signal to generate a seismocardiograph and outputting the seismocardiograph data for clinical decisions **234**.

[0053] As noted and as shown in FIG. **2**, an aspect of the quality assessment module **222** can include generating an SQI **224** of the SCG signal. The SQI **224** can be a function of the inverse distance between the SCG signal and a diverse set of reference templates. As the performance of the SQI **224** is dependent on the type of distance metric used to calculate the inverse distance between the SCG signal and a diverse set of reference templates, the disclosed technology can include dynamic-time feature matching (DTFM) as a method of distance estimation as will be described in greater detail herein.

[0054] As will be appreciated by one of skill in the art, existing methods of biosignal distance estimation, including dynamic time warping (DTW), are limited in their application. Implicit in the mapping generated by DTW are assumptions about time-series feature correspondence—namely, local minima and maxima. Since SCG waveforms are highly prone to motion-artifact noise, the assumptions made by DTW to minimize the Euclidean distance can distort the true relationships between these features and ultimately underestimate the true distance between the signals. To correct this limitation, the disclosed technology can determine that any valid mapping between an SCG signal and a template will necessarily match each feature in the template to a corresponding feature in the signal whenever possible. Because seismocardiography is highly prone to motion artifacts in ambulant subjects, the number of features in the signal will exceed the template in the vast majority of cases. In other words, because the motion sensor **102** is prone to detect motion artifacts caused by patient movement that are unrelated to cardiovascular events, the disclosed technology can be used to match features of the SCG signal to features of a template to interpret the received SCG signal data and generate a clearer seismocardiograph.

[0055] FIG. **3** illustrates a graph of distance estimation using the disclosed DTFM method **300**. As noted, the disclosed DTFM method **300** can impose additional constraints on the warp path to generate a valid warp path of the SCG signal. In certain embodiments, the DTFM method **300** can include identifying all local minima and maxima in the SCG signal **342** (such as SCG segments **220**) and a reference template **344**. The reference template **344** can be a template that is indicative of pre-recorded SCG signals having known characteristics. For example, the template **344** can be a recorded SCG signal where the location of the sensor **102** is known or an SCG signal where an underlying cardiovascular condition is known. As will be appreciated, these reference templates **344** can be pre-recorded and stored in the memory **112** of the controller **110**. Alternatively, or in addition, references templates **344** that are user-specific may be generated and stored in the memory **112**. For example, the patient **101** may be prompted or instructed to place the sensor **102** in different locations on his or her chest and one or more reference templates **344** can be generated for each position of the sensor **102** on the patient's chest. As depicted in FIG. **3**, the rows and columns of the warping matrix corresponding to timestamps of the signal **342** and template **344** features respectively are aligned with the signal **342** and the template **344**. Points lying at the intersection of these rows and columns are referred to as "intersection" points; passing the warp path through intersection points results in matching a feature in the signal **342** to a feature in the template **344**.

[0056] The DTFM method **300** can include identifying prohibited intersection points **346** in the warping matrix, as shown with crossed squares in FIG. **3**. Identifying prohibited intersection points **346** can include determining that passing the warping path through a particular point would result in either (1) matching a local minimum to a local maximum or (2) stretching the feature in the signal or template beyond some pre-defined limit. The DTFM method **300** can include removing all prohibited points **346** and denoting all remaining intersection points as "candidate" points **348**, as indicated by the solid boxes in FIG. **3**. The DTFM method **300** matches all template **344** features with a signal **342** feature, if possible, to determine an optimal warp path **350**. The DTFM method **300** can include repeating this process for each template **344** to determine the best valid warp path **350** based on the features of the template **344** and the signal **342**. Thus, valid warp paths are those that pass through a candidate point **348** associated with each template **344** feature whenever it is possible to do so—namely, whenever (1) the feature has corresponding candidate points **348** and (2) doing so would not violate pre-existing constraints. The optimal path **350** can then be chosen as the valid path that minimizes the Euclidean distance between the warped signals.

[0057] Since there generally exists only one optimal warp path **350** between any two points in the matrix—as defined by minimizing Euclidean distance—the set of valid warp paths **352** can be small in number. Because the number of valid warp paths **352** is relatively small, the DTFM method **300** can rapidly and efficiently identify all valid warp paths **352** and determine the optimal warp path **350** based on the identified valid warp paths **352**. To illustrate, in the example depicted in FIG. **3**, multiple valid warp paths **352** are depicted while only a single optimal warp path **350** is depicted. The optimal warp path **350** is chosen in part because the third maximum in the signal **342** is determined to be aberrant, and the third minimum in the signal **342** is mapped to the second minimum in the template **344** resulting in the optimal warp path's **350** route as compared to a DTW warp path's **354** route.

[0058] As described above, the SQI **224** as illustrated in FIG. **2** is a function of the inverse distance between a captured signal (e.g., signal **342**) and a reference template (e.g., template **344**), shown in the following Equation (1).

$$SQI(s,t) \triangleq \exp\left(\frac{-\lambda D(s,t)}{L(s,t)}\right) \quad \text{Equation (1)}$$

[0059] where s and t are the captured signal and reference template respectively, D(•) is the distance function, L is the length of the warped signal, and λ is an optional distance penalty. Unit SQI is achieved when there is no distance between the signals, and the SQI approaches zero exponentially as the sample-averaged distance increases. Since the length of signals (i.e., SCG signals **220**) after warping may vary, L is intended to normalize the D by the length of the signal, yielding a distance-per-datapoint. λ determines the decay rate of the exponential term and thus only influences the range in [0, 1] in which scores commonly fall.

[0060] Because the reliability of the SQI **224** is highly dependent on the quality of the template, and because there is no reference standard for seismocardiography, using a single template may not yield a valid SQI **224** for all patients. Thus, the disclosed technology can include a set of templates T={t1, t2, . . . , t|T|}. The SQI **224** can therefore be defined over the template set T as

$$\underset{\mathcal{T}}{SQI}(s) \triangleq \frac{1}{|\mathcal{T}|}\sum_{t\in\mathcal{T}} SQI(s,t) \quad \text{Equation (2)}$$

[0061] where |T| is the number of elements in set T. By increasing the size and diversity of the template set, Equation (2) provides a more reliable SQI **224**.

[0062] Using a population approach addresses the problem of determining the quality of the templates themselves. This task can be intractable both due to the lack of an objective reference standard and because template quality can vary situationally. As the number and diversity of templates increase, the influence of low-quality templates is averaged and thereby diminished, while representative templates can drive the overall SQI **224** higher or lower. As will be appreciated, this improves SQI **224** stability without incorporating subjective assumptions about template quality. Notably, scaling the score of each template by a static value—related to its quality, for instance—would not change SQI performance; though the final value can change, relative scores assigned to the signals would remain consistent, as all scores are equally affected by scalar weights.

[0063] To determine an appropriate classifier **226** for SCG signals, SCG signals drawn from a source distribution—or class—can generally result in a higher SQI from templates **344** created from the same class compared to others. If this assumption always held true, classification would be quite simple: given N classes, a template (i.e., template **344**) set can be defined as T={t1, t2, . . . , t|T|} where t_i is a template created from signals from the ith class. Classifying the input signal s can be determined by

$$C^*_{\mathcal{T}}(s) = \underset{i}{\operatorname{argmax}} SQI(s,t_i) \quad \text{Equation (3)}$$

[0064] where $C^*_T(s)$ is the class of s predicted by template set T. The selected class is therefore the value of the argument i which maximizes the SQI **224**. Since there is no known prototypical SCG signal, the classifier C^*_T may not generalize well due to its high dependence on template quality.

[0065] The system **100** can be configured to compensate for template quality variability by determining the prior likelihood of the template to give a certain SQI **224** to signals from each class. To do this, the disclosed technology can re-frame the classification problem in the above Equation (3) as

$$C_{\mathcal{T}}(s) = \underset{i}{\operatorname{argmax}} P_{Y|X}(Y=i \mid X=x) \quad \text{Equation (4)}$$

[0066] $P_{Y|X}$ is the probability that the true class of s is Y given the vector x of SQIs assigned to the signal by the template set.

[0067] Using Bayes' rule, Equation (4) is equivalent to

$$C_{\mathcal{T}}(s) = \underset{i}{\operatorname{argmax}} \frac{P_{X|Y}(X=x \mid Y=i)P_Y(Y=i)}{P_X(X=x)} = \underset{i}{\operatorname{argmax}} P_{X|Y}(X=x \mid Y=i) \quad \text{Equation (5)}$$

since x is known and one of skill in the art can assume that all classes are equiprobable. The system **100** can learn the probability distribution based on training data, a technique called Bayes estimation. The learning process can be greatly accelerated by imposing assumptions on the probability distribution; among the most common types are linear discriminant analysis (LDA), in which the distributions are assumed to be Gaussian with fixed covariance across classes; and quadratic discriminant analysis (QDA), in which the covariance restriction is lifted.

[0068] Even with Bayesian methods, accurate classification with Equation (5) still relies on the quality of the template **344** set, and thus C_T can be a weak classifier. However, predictive performance of this method can improve by using ensemble prediction. As is understood by those of skill in the art, ensemble prediction is a robust technique whereby several weak classifiers act in unison to generate stronger predictions. As predictive performance of an ensemble classifier relies on diversity of its members, methods such as bagging and boosting can also be employed during training.

[0069] As illustrated in FIG. **4**, the system **100** can be configured to apply ensemble prediction **400** to this method **300** and a superset M composed of unique template **344** sets can be used such that M={T1, T2, . . . , T|M|} where |M| is the number of template **344** sets. The method **400** can include training each classifier **460** as per Equation (5) and obtaining a majority vote **464** from the superset M of votes **462** on signal s as

$$V_M(s) = \underset{\mathcal{T}_i \in M}{\operatorname{mode}} C_{\mathcal{T}_i}(s), \quad \text{Equation (6)}$$

which returns the most common prediction **466** across all templates in set M. In other words, a template **344** set is composed of a group of templates, each derived from SCG signals belonging to a different class. Each template **344** can be used to assign the incoming signal an SQI **224**. For each template **344** set, the method **400** can include mapping the SQI **224** values to the most likely classification (classifier **460**) (accounting for variability in template **344** quality), which represents the vote **462** of the template **344** set. The system **100** then selects the prediction **466** that is the mode class (majority vote **464**) of all template set votes **462**.

[0070] As will be appreciated, by selecting diverse template **344** sets—such as by constructing each template **344** set from a different subject's data—the generalizability of this model improves, becoming less sensitive to the quality of any individual template **344**. This property is valuable in SCG signal processing, as quality templates **344** are difficult to identify.

[0071] The ensemble prediction **400**, as illustrated in FIG. **4**, also can be used by the system **100** to detect and localize sensor (e.g., motion sensor **102** and/or electrical activity sensor **104**) misplacement. For example, templates **344** can be generated and stored in the memory **112** of the controller **110** by obtaining SCG data when placing the sensor in various locations on the patient's chest. Each location can be denoted with its own individual identification (e.g., C (center), L (left), R (right), T (top), and B (bottom), etc.). Each template **344** generated at each location can have its own characteristics that can later be used to determine a location of the sensor based on the obtained SCG data.

[0072] To illustrate, using the five location indications for templates described above (i.e., C (center), L (left), R (right), T (top), and B (bottom)), multiple subject-specific templates **344** can be generated based on obtained SCG data. Each template **344** set can be composed of five templates **344**, generated from the subject's resting-period segments from each of the five accelerometer positions. Thus, the template set for each subject S can be $T_S=\{t^s_C, t^s_L, t^s_R, t^s_T, t^s_B\}$. These template sets can then combined into a superset $M=\{T1, T2, \ldots, T10\}$. A new superset M_S can then be defined based on selected subjects such that $M_S=\{Ti\}$, $i\in[1, 10]$, $i\neq S$. To use this superset for classification purposes, the prior distributions of selected subjects can be characterized to obtain C_T as described above. This setup can be analogous to treating each set as a separate QDA classifier.

[0073] For each set T_i in MS, these parameters can be learned by obtaining the SQI **224** for each template **344** t^i_j, $j\in\{C, L, R, T, B\}$. μi can then be calculated as the mean score of each template **344** t^j_j for each class **460**. Each element in Σi can be calculated as the covariance of SQIs **224** between the five templates in T_i for each class **460**, respectively. Once the prior distributions are estimated, predictions **466** can be generated for all segments for subject S using superset M_S. The predictions **466** can then be used to localize the sensor and determine whether the sensor is misplaced.

[0074] FIGS. **5**A and **5**B illustrate a method **500** of determining whether the motion sensor **102** is misplaced when mounted on a patient **101**, in accordance with the disclosed technology. The disclosed technology can include generating templates **344** for each position of the motion sensor **102**. As illustrated in FIG. **5**A, a template **344** can be generated for signals obtained by the motion sensor **102** in various positions on the patient's **101** chest.

[0075] The templates **344** can then be used to determine a position of the motion sensor **102** on the patient's **101** chest when a signal **342** is obtained by the motion sensor **102**. For example, and as will be described herein, a similarity between an obtained signal **342** and a template **344** can be computed to determine the most likely location of the motion sensor **102** on the patient's **101** chest.

[0076] As illustrated in FIG. **5**B, similarity between a signal **342** and a template **344** can be computed using the SQI **224**, including dynamic-time feature matching (DTFM), as previously described. To select an appropriate template **344**, the disclosed technology can include defining $X_{s,p}$ as a set of SCG signals for a subject (patient) $s\in S$ and position $p\in\mathcal{P}$. For each signal **342** segment $x_i\in X_{s,p}$, the average distance d_i can be calculated by the following Equation (7).

$$d_i = \frac{1}{M-1}\sum_{j=1}^{M} \mathbb{1}\{j \neq i\}\mathscr{D}(x_i, x_j) \qquad \text{Equation (7)}$$

where M is the number of signal **342** segments. The signals **342** can then be ranked based on their average distance, with lower distance representing greater fitness. The optimal template **344**, or the template **344** that minimizes Equation (7), can then be selected. By selecting a template **344**, or group of templates **344**, that best fit the signal **342**, the disclosed technology can more accurately analyze the signal **342** in comparison to the averaging-based template **344** generation previously described, and do so with less feature distortion.

[0077] Several classifiers **226** can be trained to map the feature vector of SQI **224** scores per segment to its motion sensor **102** position **566**. The classifiers **226** can include linear (LDA) and quadratic discriminant analysis (QDA); k-nearest neighbors (k-NN) with 1, 10, and 100 neighbors; and support vector machines (SVM) with linear and quadratic kernels. These models can be chosen due to their relative simplicity in terms of hyperparameter tuning.

[0078] Once the motion sensor **102** position **566** is known, an output signal can be sent to a connected user interface (e.g., user interface **118**) to indicate where the motion sensor **102** is located and whether the motion sensor **102** should be relocated. By selecting individual templates **344**, or groups of templates **344**, that best fit the signal **342**, motion sensor **102** localization can more accurately be achieved without patient-specific calibration of the motion sensor **102**.

[0079] As previously described, the morphology SCG signals can be both patient-specific and highly transient which can make obtaining relevant information from the SCG signal difficult. To help overcome these issues, the disclosed technology can include a method **600**, as illustrated in FIG. **6** and referred to as seismocardiogram generative factor encoding (SGFE), which models the SCG waveform as a stochastic sample from a low-dimensional subspace defined by a unified set of generative factors. In other words, by using SGFE, the SCG waveform can be modeled as a stochastic sample from an underlying (low-dimensional) dynamical system. Among other things, the method **600** can be used to enable algorithmic compensation for motion sensor **102** misplacement during generative factor inference to facilitate clinical outcomes 684.

[0080] For the sake of simplicity, a brief overview of the method **600** will first be described and then specific details about various elements of the method **600** will be described. As illustrated in FIG. **6**, graph **670** depicts the consistent dynamics of the Aortic Opening (AO) and Aortic Closing (AC) during periods of stress (e.g., exercise, trauma, etc.) and recovery. While the particular trajectory in this state space in response to stress can be patient-specific, the dynamic behavior is largely preserved. Various generative factors **672** can affect the recorded SCG signal. Some of these generative factors **672** can be static (i.e., anatomy, physiology, and sensor position (e.g., motion sensor **102**)) while other generative factors can be dynamic such as the hemodynamics (AO and AC) of the patient. The recorded SCG signal can be modeled as a stochastic sample **674** from these underlying generative factors **672**. As will be described in greater detail herein, the method **600** can include using the SGFE to map **676** the SCG signals to a low-dimensional subspace. As illustrated in graph **678** the SCG signals can exhibit consistent dynamics in this learned low-dimensional subspace, however observed dynamics can be dependent on the position of the motion sensor **102**. The position of the motion sensor **102** can be localized **680** using any of the previously described methods. The method **600** can further include applying position specific regression **682** to the learned subspace and the hemodynamic factors can be inferred independently from the other factors to facilitate clinical outcomes 684 for the patient.

[0081] For brevity in the following sections, shorthand will be used when describing matrices and vectors. Matrices, as described herein, are collections of row-wise vectors containing data from subsequent observations in the time interval T:=[1, T]. Consider an example T-by-M matrix of real numbers $U \in \mathbb{R}^{T \mathcal{M}}$. It can be assumed that, $U:=[u^{T}_{1} \ldots u^{T}_{T}]^{T}$ where $u_t \in \mathbb{R}^{\mathcal{M}} \forall t \in T$. In other words, U is composed of T vectors of length M, where each vector u_t is an observation at time t. Since this notation is used frequently, the shorthand $U:=\{u^{(\mathcal{M})}\}$ is used. In any such matrix, $u^{(i,j)}$ refers to the element of U in the i^{th} row and j^{th} column while $u^{(i)}{}_{t}$ refers to the i^{th} element in vector u_t. Tuples, which are ordered sequences of objects, are indicated by lists of variables enclosed by parentheses. For example, the notation V:=(U, w) is used to define the variable Vas a tuple of the matrix U and vector w.

[0082] Since the SCG signal derives from the chest wall's response to underlying events, the signal can be abstracted as

$$F \longrightarrow \boxed{R_{\Phi}(F \mid P)} \longrightarrow X_P \qquad \text{Equation (8)}$$

where $F:=\{f^{(D)}\}_T$ represents the hemodynamic generative factors of the signal **342**, R is a response function that generates the waveform, and $X_P:=\{x^{(\mathcal{M})}\}_T$ is the set of observed SCG vectors from position P. The response function R is parameterized by Φ', which represents the static generative factors **672** related to the patient's **101** anatomy and physiology, and is conditioned on the motion sensor **102** position P. Under the assumption that hemodynamic factors vary dynamically according to the state of the cardiovascular system, the factors at each timestep can be described as

$$(s_0, \Delta) \longrightarrow \boxed{G(s_0, \Delta)} \longrightarrow F \qquad \text{Equation (9)}$$

where $s_0 \in \mathbb{R}^K$ is an initial state vector, $A:=\{\delta^{(L)}\}_T$ represents changes in state at each point in the time period T, and G is a generator function that produces hemodynamic generative factors using this state information. Though the dimensionality of F and the state variables so and A are in reality unknown, acceptable values for D, K, and L in a computational model can be inferred, as will be described herein. The implications of modeling the SCG signal in this manner is that there can exist an encoder function E such that

$$X_P \longrightarrow \boxed{E_{\Phi}(X_P \mid P)} \longrightarrow (s_0, \Delta). \qquad \text{Equation (10)}$$

[0083] Given a set of observations X_P generated with Equation 8 the factors F that yielded these signals can be approximated by the system **100**. Using Equations 9 and 10, this can be accomplished via

$$X_P \longrightarrow \boxed{E_{\Phi}(X_P \mid P)} \longrightarrow (s_0, \Delta), \longrightarrow \boxed{G(s_0, \Delta)} \longrightarrow F. \qquad \text{Equation (11)}$$

While the functions E and G are unknown, learning functions experimentally that approximate this behavior can allow inference of hemodynamic generative factors.

[0084] FIG. **7** illustrates a seismocardiogram generative factor encoder (SGFE) **700** according to the disclosed technology. The input to the SGFE **700** is a sequence $X:=\{x^{(\mathcal{M})}\}$ of T consecutive heartbeat-separated SCG signals **342** with length M.

[0085] To compress the signals, each signal $x_t \in X$ is processed with the multi-layer convolutional network **786**. This network **786** is composed of N=6 convolution blocks in series, which convolve the signal with each of k_n filters (kernels) of length i_n in the nth block with unit step. Convolutional networks **786** can be used in cardiovascular signal processing due to the temporal dependence of time-series data. The outputs of each convolution layer can be normalized before application of an exponential linear unit (ELU) activation function. Dropout regularization with a rate of 0.2 can be imposed on the output of the activation function. Dimensionality reduction can be induced by gradually decreasing the number of filters (k_n=[64, 64, 32, 32, 16, 16]) and max pooling, which down-samples each signal by a factor of two. To accommodate for shorter signals, the kernel length can also be decreased (4=[7, 5, 5, 3, 3, 2]). The layers in this network are time-distributed, meaning the same operation can be performed for each signal $x_t \in X$.

[0086] Before modeling the dynamics present in X, the outputs of the compression network are flattened and passed through a dense "read-in" layer **787** with 64 input units, 2 (K+L) output units, and rectified linear unit (ReLU) activation with dropout regularization at a rate of 0.2. The read-in **787** and read-out **796** layers—also called mapping layers—

exist because generative factors **795** can present differently as signal features across patients. Thus, though the subspace defined by the generative factors can be conserved, mapping into and out of this subspace can require compensation for signal heterogeneity by fitting these layers on a session-specific basis. In other words, the mapping layers capture anatomical and physiological differences—represented by Φ' in Equations 8, 10, and 11—so that the dynamic model can focus on inferring factors that are common to the population.

[0087] Modeling dynamics requires estimation of the initial state so and change in state at each timestep A. As shown in FIG. **7**, the former can be computed by the system **100** with a bi-directional long short-term memory (LS™) network **788** E_Z, where the output is the average between the final outputs of the forward and backward layers. The latter can also be computed by the system **100** with a bi-directional LS™ network **789** E_Δ, where an output δ_t is produced at each timestep as the average output between the forward and backward cells. However, since this can be a VAE instantiation, these values are not evaluated explicitly; rather, they are drawn from a Gaussian distribution, the parameters of which are explicitly evaluated. Thus, the output of E_Z is a tuple **790** (μ_0, σ_0), μ_0, $\sigma_0 \in R^K$. The output of E_Δ at each timestep $t \in T$ is a tuple **791** ($\mu_{\delta,t}$ $\sigma_{\delta,t}$), $\mu_{\delta,t} \in R^L$. The i^{th} element of the initial state vector s_0 is then sampled from

$$s_0^{(i)} \sim \mathcal{N}(\mu_0^{(i)}, \sigma_0^{(i)}) \forall i \in [1, K]. \quad \text{Equation (12)}$$

where $N(\mu,\sigma)$ is a Gaussian distribution with mean μ and standard deviation σ. Similarly, at each timestep t, the j^{th} element of the state change vector dt is sampled from

$$\delta_t^{(j)} \sim \mathcal{N}(\mu_{\delta,t}^{(j)}, \sigma_{\delta,t}^{(j)}) \forall j \in [1, L], t \in \mathcal{T}. \quad \text{Equation (12)}$$

Note that each element in s_0 **792** and δ_t **793** is drawn independently. The probabilistic nature of the VAE yields a structured latent space, as nearby points will produce inherently similar outputs.

[0088] The generator network **794** can estimate the generative factors at each timestep based on the system state. The generator network **794** can be a uni-directional LS™ network, outputting a vector of factors $f_t \in R^D$ at each step t. As before, these factors **795** can be passed through a read-out **796** dense layer with D inputs and 64 outputs, which maps the generative factors **795** to corresponding signal features. Like the read-in layer **787**, this mapping can be learned on a session-specific basis to account for changes in factor manifestation as signal features.

[0089] The translated factors can be used to construct the output signals $\tilde{X} := \{\tilde{x}^{(M)}\}_T$ with the decompression network **797**. The decompression network **797** can be a mirror-image of the compression network **786**, with the number and length of kernels applied in the reverse order and up-sampling by a factor of two rather than max pooling. The output of the decompression network **797** can be a convolution layer **798** with a single filter ($k^*=1$) with length $l^*=l_1$ such that the output is a single vector at each timestep. As will be appreciated by one of skill in the art, as more data is obtained from a patient, the data can be used to update the SGFE **700** model and infer generative factors **795** concurrently.

[0090] For visual analysis of subspace behavior, the goal of the following method can be to identify the pair of dimensions in the learned subspace F that encoded the most consistent linear trajectories. Linear trajectories can be expected to arise in the latent space because, as will be illustrated, AO and AC can be found experimentally to follow linear trends in exercise-recovery when plotted against one another.

[0091] To illustrate, for each session in a test set defined by the subject $S \in [1, 10]$ and sensor (e.g., sensor **102**) position $P \in \{C, L, R, T, B\}$, the subspace mapping $F \in R^{T \times D}$ for each of $N_{S,P}$ samples in a session can be concatenated to form the matrix $F_{S,P} \in R^{T N S,P \times D}$. In this manner, each matrix $F_{S,P}$ can contain the subspace encoding of all data for one of the sessions in the test set. These matrices can be further concatenated row-wise across all subjects to form the matrix F p for each sensor (e.g., motion sensor **102**) position. Thus, F_P can contain the subspace encoding of all data from sessions from a particular sensor position.

[0092] For illustrative purposes, the following can then be performed for all P. For each pair of column vectors $(f_i, f_j) \in F_P$, $i \neq j$, linear regression can be used to find the optimal linear fit between f_i and f_j. The pair i, j in which the coefficient of determination (R^2) of the linear fit averaged across all P was maximal can be selected as the optimal axis pair for further analysis. Subspace trajectories can be visualized by plotting the resultant vectors f_1 and f_2 against one another.

[0093] A second qualitative analysis can be performed to determine whether the identified dimensions can contain useful information about the known generative factors AO and AC. An ICG-derived rAO interval can be plotted against the rAC interval on a scatter plot. Best-fit lines can then be overlaid on data from each subject to better visualize the trajectories of these intervals. For the same subjects, the subspace mappings f_1 and f_2 from the same session for the central sensor location can be plotted on a scatter plot. Best-fit lines can be overlaid on the subspace encoding for each patient in order to observe whether changes in rAO/rAC trajectories can be reflected by the identified dimensions.

[0094] Though the hyperplane defined by f_1 and f_2 can be a suitable subspace in which to observe the consistent dynamics of SCG signals, it can be sub-optimal for visualizing the effects of changing motion sensor **102** state on observed dynamics. To do so more effectively, principal component analysis (PCA) can be used to find an informative three-dimensional representation of the subspace F, and the average trajectory for each motion sensor **102** position can be plotted in these PCA dimensions for visualization.

[0095] To do so, the matrix F p can be concatenated across positions by the system **100** to form $F_{tot} \in R^{T\ Ntot \times D}$ where N_{tot} is the total number of samples in the testing set. The matrix F_{tot} thus can contain the subspace mappings for all samples in the testing set. PCA can then be performed on F_{tot} to obtain the transformation $A \in R^{D \times D}$ mapping dimensions of F_{tot} into the orthogonal subspace defined by PCA dimensions.

[0096] The following can then be performed by the system **100** for each matrix $F_{S,P}$, which can contain the subspace encoding for the session with subject S and position P. Each of the **10** matrices $F_{S,P}$, $S \in [1, 10]$ can be averaged element-wise to obtain a session-averaged matrix F_P. F_P can thereby contain the subspace encoding for position P averaged across all subjects. Subsequently, this matrix can be transformed using the matrix A to obtain $A_P = F_P A$, the mapping of F_P in the PCA subspace. Finally, for each position, the first three dimensions of A_P can then be plotted on a scatter plot for visualization (e.g., output to the user interface **118**).

[0097] FIG. **8** depicts subspace mappings **800** of recovery-period SCG data for two example patients **101**. The rows of the FIG. **8** represent each of the five different sensor positions previously described (e.g., C, L, R, T, B). From the first and last columns of FIG. **8**, it is apparent that signal morphology between the patients—and even at different sensor locations for the same patient—can vart substantially. This time-domain variability is juxtaposed with trajectories in the learned subspace which are largely conserved. Specifically, the subspace mapping of the signal during this period can follow an approximately linear trajectory in the reference frame defined by the selected subspace dimensions f_1 and f_2.

[0098] The left and right columns of FIG. **8** show a subset of the amplitude-normalized SCG data from patients 1 and 2 respectively, with the second and third columns showing the corresponding subspace trajectories respectively. The axes represent learned subspace dimensions f_1 and f_2. The small gray points in the figure represent subspace mappings with the same sensor position from the remaining patients in the testing set. Trajectory directions are overlaid (black, dotted). The indication A.U. represents arbitrary units.

[0099] FIG. **9**A represents ICG-derived AO and AC points during exercise-recovery for five example patients in a test set. AO and AC are shown as scatter points while best-fit lines for the scatter points are overlaid as dashed lines. FIG. **9**B illustrates subspace trajectories in dimensions f_1 and f_2 from centrally-placed sensors (e.g., motion sensor **102**) for the same patients. Subspace mappings are similarly shown as scatter points with best-fit lines overlaid as dashed lines. FIG. **9**C illustrates trajectories in PCA dimensions of F for SCG signals from each of the five motion sensor **102** positions averaged across all patients. The positions include center, left, right, top, and bottom. The trajectories are also indicated with black dashed lines. As will be appreciated by one of skill in the art, the disclosed technology can enable position-specific mapping to infer hemodynamic variables as illustrated in FIG. **9**C.

[0100] As illustrated in FIG. **10**, the disclosed technology can include a method **1000** of determining physiological changes during hemorrhage and subsequent fluid resuscitation via PEP estimation. As will be described in greater detail herein, the method **1000** can be used to detect and analyze low-dimensional manifold structures of SCG signals during periods of hemodynamic change. Displacement along the manifold can be linearly-related to changes in PEP and used to determine a hemodynamic change of the patient's **101** body.

[0101] The motion sensor **102** can obtain SCG signals **220** when mounted to a patient's **101** chest during periods of hemodynamic change **1010**. The SCG signals **220** can be processed by the SQI **224** previously described (illustrated as quality indexing in FIG. **10**) to remove low-quality signals. The SCG signals **220** can be compared to a manifold structure inherent to SCG signals **220** by non-linearly mapping the SCG signals **220** to positions along the low-dimensional manifold **1012** to infer hemodynamic changes. Linear dimensionality reduction with PCA can be used to visualize the manifold structure inherent to SCG signals **220**. As will be described in greater detail herein, nonlinear dimensionality reduction, such as either an ISOMAP **1014** or a manifold approximation **1016**, can be used to analyze the distance traveled along manifold to infer hemodynamic changes. For example, a computation of the displacement **1018** along the manifold can be used to determine (or infer) the hemodynamic changes **1010** of the patient **101**. As will be appreciated by one of skill in the art, the disclosed technology can be used to non-invasively detect potentially harmful or dangerous cardiac or hemodynamic changes of the patient **101**. For example, as described further herein, the disclosed technology can be used to create a graph that can be used to detect hemodynamic changes such as blood loss from a hemorrhage as illustrated in FIGS. **11**A-**11**E. For this reason, the disclosed technology can be used for reliable physiological estimation from SCG signals during trauma-induced hemorrhage and subsequent treatment. Namely, estimating indicators of cardiomechanical function such as PEP noninvasively can enable new clinical tools to allow healthcare providers to manage trauma injury, serving as additional indicators of the severity of hemorrhage and the patients' response to fluid resuscitation.

[0102] The disclosed technology can include using an ISOMAP **1014** algorithm to learn and re-embed the manifold. As illustrated in FIGS. **11**A-**11**C, a graph can be constructed from a sub-sampling of points $G_i=\{g_1, g_2, \ldots, g_L\}$ from the overall dataset $X_i=\{x_1, x_2, \ldots, x_M\}$, which form the nodes of the graph. A connection between nodes g_j and g_k can be formed if and only if there exists a point x_1 in the original dataset whose nearest neighbors are g_j and g_k as per the Euclidian distance. The geodesic distance between each pair of nodes g_j, $g_k \in Gi$ can then estimated by computing the shortest path between each pair of nodes that traverses the graph's connections. This can be performed, for example, by the Floyd-Warshall algorithm.

[0103] The manifold can then be re-embedded by the system **100** to learn a mapping $f:R^{L\times N}\rightarrow Y$ from the observation space of G_i to a lower-dimensional space $Y=R^{L\times D}$ which preserves the geodesic distances between pairs of points in the graph. As an example, "classical" multidimensional scaling (MDS) to learn this mapping. Specifically, MDS can minimize the loss function

$$L(f, G_i) = \left(\frac{\sum_{j,k} \left(d_Y^{jk} - d_G^{jk}\right)^2}{\sum_{j,k} \left(d_Y^{jk}\right)^2} \right)^{1/2}, \qquad \text{Equation (14)}$$

where $d^{jk}{}_Y = \|f(g_j) - f(g_k)\|_2$ is the Euclidian distance (or the l_2-norm) between $f(g_j)$ and $f(g_k)$ in the output space Y and $d^{jk}{}_G$ is the estimated Euclidian distance between the feature vectors g_j and g_k.

[0104] To obtain an accurate embedding of SCG manifolds the SQI **224** can first be applied by the system **100** to the SCG data to remove outliers. As the final step of processing, the latent variable Δy can be obtained by the system **100** for each patient by computing the offset of each element in $y_i^{(1)}$ from the initial element in the vector $y_i^{(1)}(0)$, such that $\Delta y_i = y_i^{(1)} - y_i^{(1)}(0)$. This can be done in order to obtain the displacement **1018** of each point on the manifold rather than the absolute position. This latent variable can be used to estimate the change in PEP (APEP) via linear regression.

[0105] Alternatively, or in addition, manifold approximation **1016** can be used by the system **100** to learn and re-embed the manifold as illustrated in FIGS. **11**D-**11**E. For each patient **101**, a separate PCA transformation can be learned from the data obtained from other patients **101** (Xi^-)

and applied to the data from the held-out patient (Xi). The initial sample from the patient **101** can then be mapped to the nearest point on a unit circle in the plane of PC**1** and PC**2**, centered at the origin. Each subsequent point can then also be mapped to the nearest point on the unit circle, and the angular offset between the new point and the initial point can be recorded. This can result in a vector $\Delta\theta_i$ containing the angular offset for each SCG signal in X_i. This process can also be repeated with an SQI cutoff increasing from 0% to 20% in increments of 5%. The latent variable $\Delta\theta$ can then be used to estimate APEP in an analogous manner to Δy from ISOMAP **1014**. Unlike the ISOMAP **1014** algorithm, the manifold approximation **1016** algorithm has $O_{(N)}$, and is thereby much more rapid.

[0106] As will be appreciated, the methods described herein can be varied in accordance with the various elements and implementations described herein. That is, methods in accordance with the disclosed technology can include all or some of the steps described above and/or can include additional steps not expressly disclosed above. Further, methods in accordance with the disclosed technology can include some, but not all, of a particular step described above. Further still, various methods described herein can be combined in full or in part. That is, methods in accordance with the disclosed technology can include at least some elements or steps of a first method and at least some elements or steps of a second method.

[0107] While the present disclosure has been described in connection with a plurality of example aspects, as illustrated in the various figures and discussed above, it is understood that other similar aspects can be used, or modifications and additions can be made to the described subject matter for performing the same function of the present disclosure without deviating therefrom. In this disclosure, methods and compositions were described according to aspects of the presently disclosed subject matter. But other equivalent methods or compositions to these described aspects are also contemplated by the teachings herein. Therefore, the present disclosure should not be limited to any single aspect, but rather construed in breadth and scope in accordance with the appended claims. Moreover, various aspects of the disclosed technology have been described herein as relating to methods, systems, devices, and/or non-transitory, computer-readable medium storing instructions. However, it is to be understood that the disclosed technology is not necessarily limited to the examples and embodiments expressly described herein. That is, certain aspects of a described system can be included in the methods described herein, various aspects of a described method can be included in a system described herein, and the like.

What is claimed is:

1. A method of detecting morphological changes using a wearable cardiac monitor, the method comprising:
- receiving seismocardiographic data from a motion sensor;
- determining, based at least in part on the seismocardiographic data, a classifier of the seismocardiographic data;
- determining, based at least in part on the seismocardiographic data, a signal quality index of the seismocardiographic data;
- determining, based on the classifier and the signal quality index, a quality of the seismocardiographic data; and
- outputting, to a graphical user interface, the quality of the seismocardiographic data.

2. The method of claim **1**, wherein the classifier comprises multiple classifiers, and wherein the method further comprises:
- performing ensemble prediction by utilizing the multiple classifiers to create an ensemble classifier.

3. The method of claim **1** further comprising:
- retrieving a reference template, the reference template comprising representative seismocardiographic data; and
- determining the signal quality index by determining a distance between the seismocardiographic data and the reference template.

4. The method of claim **3** further comprising:
- estimating the distance between the seismocardiographic data and the reference template by dynamic-time feature matching, wherein dynamic-time feature matching comprises:
  - determining a local minimum and a local maximum of the seismocardiographic data;
  - determining a local minimum and a local maximum of the reference template;
  - determining a prohibited intersection point;
  - determining a candidate point; and
  - generating a warp path through the candidate point.

5. The method of claim **1** further comprising:
- retrieving a location-specific reference template, the location-specific reference template comprising representative seismocardiographic data at a predetermine location; and
- determining a location of the motion sensor by at least determining a distance between the seismocardiographic data and the location-specific reference template.

6. The method of claim **5** further comprising:
- performing a seismocardiogram generative factor encoding;
- comparing the seismocardiographic data to a low-dimensional subspace; and
- applying a position-specific regression to the low-dimensional subspace to determine a hemodynamic factor.

7. The method of claim **5** further comprising:
- comparing the seismocardiographic data to a low-dimensional manifold;
- performing a manifold approximation to analyze a distance traveled along the low-dimensional manifold; and
- determining a hemodynamic change based on the distance traveled along the low-dimensional manifold.

8. A wearable cardiac monitoring system comprising:
- a motion sensor configured to detect movement of a user's chest and output seismocardiographic data; and
- a non-transitory, computer-readable medium having instructions stored thereon that, when executed by one or more processors, cause a controller to:
  - receive the seismocardiographic data from the motion sensor;
  - determine, based at least in part on the seismocardiographic data, a classifier of the seismocardiographic data;
  - determine, based at least in part on the seismocardiographic data, a signal quality index of the seismocardiographic data;
  - determine, based on the classifier and the signal quality index, a quality of the seismocardiographic data; and

output, to a graphical user interface, an indication of the quality of the seismocardiographic data.

9. The wearable cardiac monitoring system of claim **8**, wherein the classifier comprises a property of a source distribution of the seismocardiographic data.

10. The wearable cardiac monitoring system of claim **8**, wherein the classifier comprises multiple classifiers, and

wherein the instructions, when executed by the one or more processors, further cause the controller to:

perform ensemble prediction by utilizing the multiple classifiers to create an ensemble classifier.

11. The wearable cardiac monitoring system of claim **8**, wherein the instructions, when executed by the one or more processors, further cause the controller to:

retrieve a reference template, the reference template comprising representative seismocardiographic data; and

determine the signal quality index by determining a distance between the seismocardiographic data and the reference template.

12. The wearable cardiac monitoring system of claim **11**, wherein the instructions, when executed by the one or more processors, further cause the controller to:

estimate the distance between the seismocardiographic data and the reference template by dynamic-time feature matching.

13. The wearable cardiac monitoring system of claim **12**, wherein dynamic-time feature matching comprises:

determining a local minimum and a local maximum of the seismocardiographic data;

determining a local minimum and a local maximum of the reference template;

determining a prohibited intersection point;

determining a candidate point; and

generating a warp path through the candidate point.

14. The wearable cardiac monitoring system of claim **8**, wherein the instructions, when executed by the one or more processors, further cause the controller to:

retrieve a location-specific reference template, the location-specific reference template comprising representative seismocardiographic data at a predetermine location; and

determine a location of the motion sensor by at least determining a distance between the seismocardiographic data and the location-specific reference template.

15. The wearable cardiac monitoring system of claim **14**, wherein the instructions, when executed by the one or more processors, further cause the controller to:

perform a seismocardiogram generative factor encoding;

compare the seismocardiographic data to a low-dimensional subspace; and

apply a position-specific regression to the low-dimensional subspace to determine a hemodynamic factor.

16. The wearable cardiac monitoring system of claim **14**, wherein the instructions, when executed by the one or more processors, further cause the controller to:

compare the seismocardiographic data to a low-dimensional manifold;

perform a manifold approximation to analyze a distance traveled along the low-dimensional manifold; and

determine a hemodynamic change based on the distance traveled along the low-dimensional manifold.

17. The wearable cardiac monitoring system of claim **8**, wherein the controller is configured to wirelessly receive the seismocardiographic data from the motion sensor.

18. The wearable cardiac monitoring system of claim **17**, wherein the controller is a remote server configured to wirelessly receive the seismocardiographic data from the motion sensor.

19. The wearable cardiac monitoring system of claim **8**, wherein the controller is integrated with the motion sensor into a single wearable device.

20. The wearable cardiac monitoring system of claim **8**, wherein the instructions, when executed by the one or more processors, further cause the controller to:

receive a first input to change a threshold value of the classifier; and

receive a second input to change a threshold value of the signal quality index.

* * * * *